Activity-Based Profiling of a Physiologic Aglycone Library Reveals Sugar Acceptor Promiscuity of Family 1 UDP-Glucosyltransferases from Grape[1][W]

Friedericke Bönisch[2], Johanna Frotscher[2], Sarah Stanitzek[2], Ernst Rühl, Matthias Wüst, Oliver Bitz, and Wilfried Schwab*

Biotechnology of Natural Products, Technische Universität München, 85354 Freising, Germany (F.B., W.S.); Geisenheim University, Department of Grape Breeding, 65366 Geisenheim, Germany (J.F., E.R., O.B.); and Food Chemistry Research Unit, Institute of Nutrition and Food Sciences, University of Bonn, D–53115 Bonn, Germany (S.S., M.W.)

ORCID ID: 0000-0002-9753-3967 (W.S.).

Monoterpenols serve various biological functions and accumulate in grape (*Vitis vinifera*), where a major fraction occurs as nonvolatile glycosides. We have screened the grape genome for sequences with similarity to terpene URIDINE DIPHOSPHATE GLYCOSYLTRANSFERASES (UGTs) from Arabidopsis (*Arabidopsis thaliana*). A ripening-related expression pattern was shown for three candidates by spatial and temporal expression analyses in five grape cultivars. Transcript accumulation correlated with the production of monoterpenyl β-D-glucosides in grape exocarp during ripening and was low in vegetative tissue. Targeted functional screening of the recombinant UGTs for their biological substrates was performed by activity-based metabolite profiling (ABMP) employing a physiologic library of aglycones built from glycosides isolated from grape. This approach led to the identification of two UDP-glucose:monoterpenol β-D-glucosyltransferases. Whereas VvGT14a glucosylated geraniol, *R*,*S*-citronellol, and nerol with similar efficiency, the three allelic forms VvGT15a, VvGT15b, and VvGT15c preferred geraniol over nerol. Kinetic resolution of *R*,*S*-citronellol and *R*,*S*-linalool was shown for VvGT15a and VvGT14a, respectively. ABMP revealed geraniol as the major biological substrate but also disclosed that these UGTs may add to the production of further glycoconjugates in planta. ABMP of aglycone libraries provides a versatile tool to uncover novel biologically relevant substrates of small-molecule glycosyltransferases that often show broad sugar acceptor promiscuity.

Plant secondary metabolites are frequently decorated with Glc that is transferred from uridine diphosphoglucose by a so-called family 1 URIDINE DIPHOSPHATE GLUCOSYLTRANSFERASE (UGT; Caputi et al., 2012). Since the glucosylation process can be envisaged as a simple nucleophilic displacement reaction of Second-order Nucleophilic Substitution type, the product is a β-glucoside. A remarkably large array of different small molecules is glucosylated in planta, including terpenoids, alkaloids, cyanohydrins, and glucosinolates, as well as flavonoids, isoflavonoids, anthocyanidins, and phenylpropanoids. In grape (*Vitis vinifera*) alone, more than 200 different glucosides have been identified, and there is special interest in those glucoconjugates, which can contribute to wine flavor after the hydrolytic release of volatiles during the biotechnological vinification sequence leading from grape to aged wine (Wirth et al., 2001). These flavorless glucoconjugates accumulate in grape berries during maturation and can be grouped according to their linked aglycones into monoterpenes, C13-norisoprenoids, aliphatic alcohols, and shikimate-derived benzoids and phenylpropanoids (Sefton et al., 1996). It still remains an open question how this large number of structurally different flavor precursors is actually glucosylated in vivo, because the in vitro activities of single UGTs show large differences in the individual range of acceptors. Some UGTs are considered highly specific with respect to substrate specificity, regiospecificity, and stereospecificity, whereas others glucosylate a broad range of acceptors (Osmani et al., 2009). The latter phenomenon is called promiscuity and could decisively contribute to the immense structural variations of small plant secondary metabolites regarding their glucosylation pattern (Schwab, 2003). Biochemical characterization of the substrate specificity of the UGTs, therefore, is a major challenge that scientists face when approaching the study of the actual biological function of these enzymes, whose number of available sequences is rapidly increasing as a result of EST and genome sequencing programs.

The potential broad substrate preference of many UGTs requires a wide range of substrates to be tested, which is often impeded by a biased collection of acceptor molecules. This problem was recently alleviated by the application of the so-called activity-based metabolic profiling (ABMP) approach (Duckworth and Aldrich, 2010). ABMP allows unbiased discovery of enzymatic

[1] This work was supported by the Deutsche Forschungsgemeinschaft (grant no. DFG SCHW634/17).

[2] These authors contributed equally to the article.

* Address correspondence to schwab@wzw.tum.de.

The author responsible for distribution of materials integral to the findings presented in this article in accordance with the policy described in the Instructions for Authors (www.plantphysiol.org) is: Wilfried Schwab (schwab@wzw.tum.de).

[W] The online version of this article contains Web-only data.
www.plantphysiol.org/cgi/doi/10.1104/pp.114.242578

 © 2014 American Society of Plant Biologists. All Rights Reserved.

activities encoded by genes of unknown function and applies chromatographic techniques to analyze the impact of a recombinant enzyme on the homologous cellular extract as the most physiologic chemical library of potential substrates and products (de Carvalho et al., 2010). Notably, it provides a synthesis and label-free approach that circumvents the unavailability of a complete set of relevant substrate molecules. We have adapted this powerful technique to probe the substrate specificity of heterologously expressed UGTs whose sequences were obtained from the grape genome database. A grape berry aglycone library was prepared by isolation and subsequent enzymatic hydrolysis of grape glycoconjugates. Incubation of the liberated aglycones with the recombinant UGTs yielded glucosides that were separated from the unreacted free aglycones by extraction and were identified by complementary gas chromatography-mass spectrometry (GC-MS) and liquid chromatography-mass spectrometry (LC-MS) techniques. This approach allowed the identification of UDP-Glc:monoterpenol β-D-glucosyltransferases that are characterized by the glucosylation of a rather broad monoterpenol spectrum and complemented with considerable activities toward aliphatic alcohols and benzoic compounds. Gene expression analyses in combination with metabolite analysis confirmed their biological functions.

RESULTS

Expression Analysis: Temporal and Spatial

The most prominent terpene compounds occurring generally and in high concentrations in aroma-related grapes (e.g. cv Muscat a petits grains blanc FR 90, hereafter referred to as 'Muscat') and wines are geraniol, nerol, citronellol, α-terpineol, and linalool (Fig. 1). To identify UGT genes that are likely to contribute to the glucosylation of these terpenols during grape ripening, we screened the grape cv Pinot Noir genome for sequences with substantial identity to monoterpene UGTs found in Arabidopsis (*Arabidopsis thaliana*; Caputi et al., 2008, 2010). Seven putative *VvGT* genes (*VvGT14*, VIT_18s0001g06060; *VvGT15*, VIT_06s0004g05780; *VvGT16*, VIT_03s0017g01130; *VvGT17*, VIT_18s0001g05950; *VvGT18*, VIT_03s0180g00280; *VvGT19*, VIT_18s0001g05910; and *VvGT20*, VIT_05s0062g00430) were selected (Fig. 2; for genome location, see Supplemental Fig. S1), and their transcript levels were analyzed using GenomeLab Genetic Analysis System (GeXP) profiling in two cultivars in three different vegetative tissues (Fig. 3; Supplemental Fig. S2) and in grape berry exocarp of five cultivars at different developmental stages (Fig. 4; Supplemental Fig. S3). In nonberry tissue (inflorescence, leaf, and root), *VvGT14* and *VvGT15* showed the lowest relative transcript levels of the seven putative UGT genes but displayed a ripening-related expression pattern in berry skins similar to *VvGT16*. A significant amount of *VvGT14* to *VvGT16* mRNA was found in berry exocarp at late stages of berry ripening (Fig. 4). Notably, their transcript levels differed considerably between cultivars. *VvGT14* was expressed primarily in the two surveyed clones of 'White Riesling' (cv White Riesling 239-34 Gm and White Riesling 24-196 Gm), *VvGT15* in 'Muscat', and *VvGT16* in the two clones of 'Gewurztraminer', cv Gewurztraminer FR 46-107 and Gewurztraminer 11-18 Gm. In contrast,

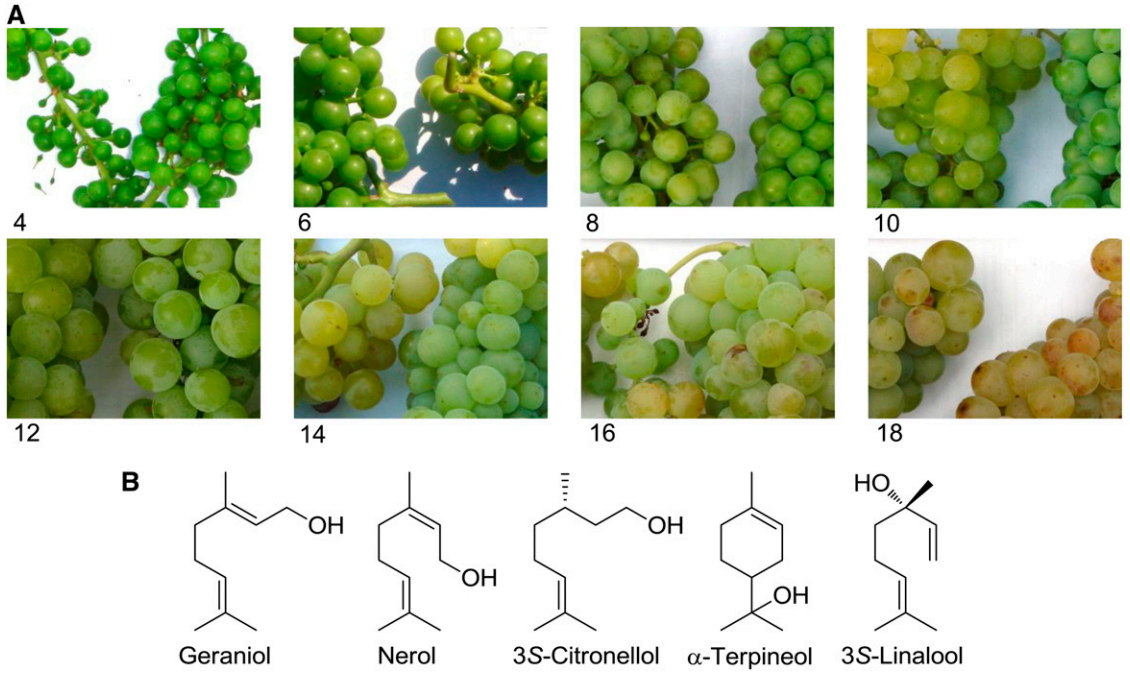

Figure 1. Grapes of 'Muscat' (A) and major monoterpenols found in grape (B). Photographs were taken every 2 weeks between week 4 and week 18 after flowering. The width of the photographs is 10 cm.

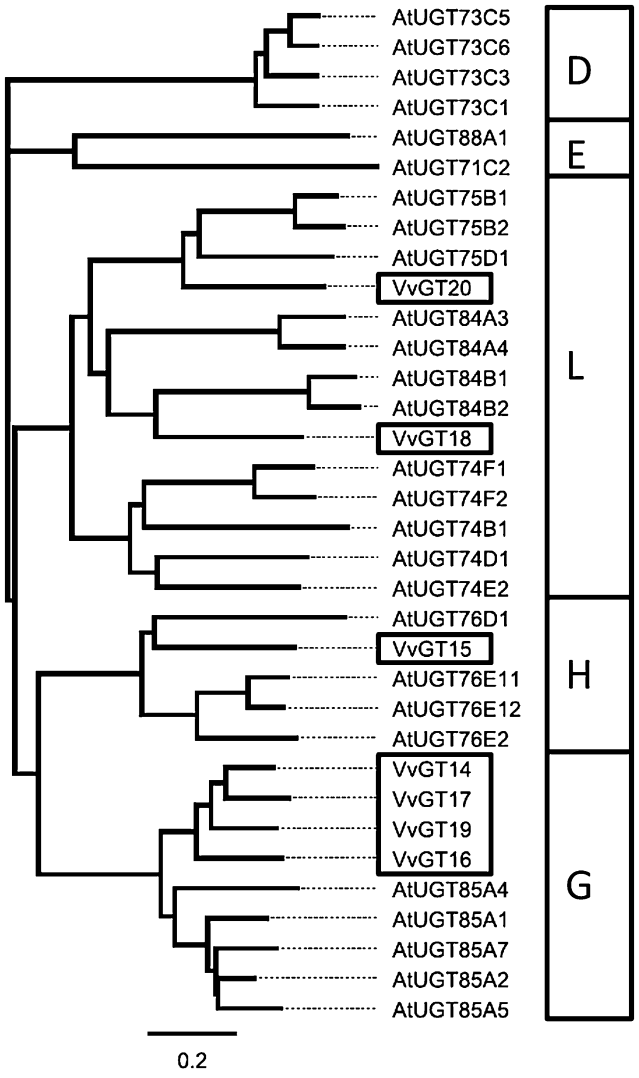

Figure 2. Phylogenetic tree of glucosyltransferase protein sequences. Protein sequences from Arabidopsis (AtUGT) with known glucosyltransferase activity toward terpenes are also shown. VvGT14 to VvGT20 were investigated in this study. Glucosyltransferase subgroup assignment is shown in the boxes at right.

VvGT17 to *VvGT20* transcripts accumulated to comparatively high levels in inflorescence, leaf tissue, and immature green berries (Supplemental Fig. S2), but their amounts decreased after veraison (the onset of ripening; Supplemental Fig. S3). The expression patterns of *VvGT17* to *VvGT20* were very similar in all analyzed cultivars (Supplemental Fig. S3). Expression profiling was also performed for berry skins of 'Muscat' in two subsequent years. In 2011, in comparison with 2012, similar relative transcript levels of *VvGT14* and *VvGT15* were reached, but slightly later (2–3 weeks; Supplemental Fig. S4). The same is true for the ripening-related parameters sugar content and pH value. However, this effect was not observed for *VvGT17* to *VvGT20*, as their relative expression levels are negligible at the start of ripening (10–12 weeks after flowering; Supplemental Fig. S4). Thus, *VvGT14* to *VvGT16* appear to play an important role in grape berry ripening, as their expression levels peak after veraison and they are barely expressed in other tissues, except *VvGT16*.

Metabolite Profiling

To correlate the expression profiles of putative UGTs with terpenyl glucoside concentration, we performed metabolite analysis in five cultivars during grape ripening (Table I). Solid-phase extraction was used to isolate free (nonglycosylated) and glycosylated monoterpenes from grape skins (exocarp) of various grapevine cultivars (Gunata et al., 1988; Mateo and Jiménez, 2000). Since grape skins (exocarp) accumulate the majority of terpene metabolites detected in grape berries, they were separated from the flesh and extracted (Wilson et al., 1986). The main monoterpenes of grape (geraniol, nerol, linalool, and citronellol) were quantified by GC-MS analysis, whereas their nonvolatile monoterpenyl glucosides were determined by a stable isotope dilution analysis method using HPLC-tandem mass spectrometry (MS/MS). Isotopically labeled internal standards were chemically synthesized. Grape berries of the grape cultivars differed not only in their amounts of total terpenes but also in their terpene profiles at different developmental stages (Table I). Monoterpenols (free and glucosidically bound) were hardly detected (less than 0.25 mg kg^{-1} grape skins) in grape exocarp of 'Gewurztraminer FR 46-107', probably due to the impaired monoterpene biosynthesis of this clone. 'Gewurztraminer 11-18 Gm' and 'Muscat' skins accumulated significant levels of geraniol, citronellol, and nerol derivatives (up to 5.5 mg kg^{-1} grape skins) and displayed a heterogenous spectrum of monoterpenes at every stage of ripening. Both 'White Riesling' clones produced smaller amounts of the metabolites that were mainly observed at weeks 15 to 17. In general, the highest concentration of free and bound terpenols was found in the late stages of ripening in all investigated cultivars, whereupon geraniol and its β-D-glucoside were the predominant terpene metabolites. The ratios of the amounts of free to glucosidically bound forms of individual monoterpenes varied considerably at weeks 15 and 17 after flowering. These values provide a first indication of variable UGT activity in different cultivars and/or differential preference of the UGTs for their monoterpene substrates. Notably, the evolution of monoterpenyl β-D-glucosides in grape exocarp of the 'White Riesling' clones (Table I) correlated well with the expression pattern of *VvGT14* in the same tissue (Fig. 4). While significant transcript levels were only detected at week 11 after flowering, remarkable levels of the glucosides were not found until week 13. In contrast, the time course of *VvGT15* mRNA levels in 'Muscat' coincided with the terpenyl glucoside concentrations in the same clone, as considerable amounts of transcripts and glucosides were found throughout weeks 6 to 17 after flowering. At the very late stages of ripening (weeks 15–17),

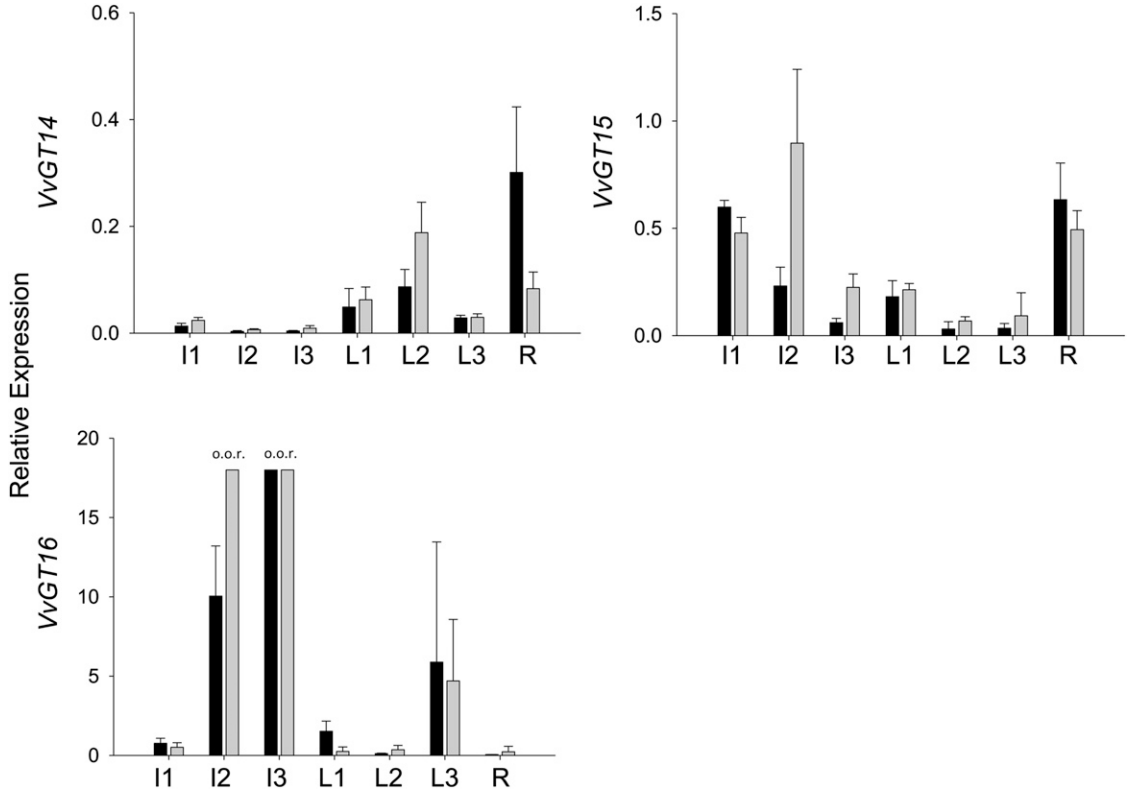

Figure 3. Gene expression analysis of *VvGTs* by GeXP in nonberry tissues. The relative expression was quantified in 'Gewurztraminer 11-18 Gm' (black bars) and 'White Riesling 239-34 Gm' (gray bars). Sampled tissues were inflorescences at 4 weeks (I1) and 2 weeks (I2) before flowering and at full bloom (I3), leaves at the ages of approximately 1 week (L1), 3 weeks (L2), and 5 weeks (L3), and roots (R). Mean values + SD of three independent experiments are shown. o.o.r., Out of range.

the expression of *VvGT16* increased strongly in 'Gewurztraminer 11-18 Gm', a cultivar that produced a high concentration of geranyl β-D-glucosides.

Heterologous Expression of *VvGT14*, *VvGT15*, and *VvGT16* and Enzymatic Activity

The alleles of *VvGT14a* to *VvGT14c*, *VvGT15a* to *VvGT15c*, and *VvGT16* were isolated from grape cultivars and cloned in the expression vector pGEX-4T-1. The recombinant proteins were expressed in *Escherichia coli* with an N-terminal glutathione *S*-transferase (GST) tag, affinity purified, and verified by SDS-PAGE and western blot using a GST-specific antibody (Supplemental Figs. S5 and S6). Enzyme activity studies were performed with UDP-[^{14}C]Glc and various putative substrates (terpenols, flavonoids, and different monoalcohols) that are known to be glycosidically bound and present in grape (Gunata et al., 1988; Voirin et al., 1990; Sefton et al., 1996; Ford and Hoj, 1998; Wirth et al., 2001). Recombinant VvGT14a, VvGT15a to VvGT15c, and VvGT16 converted several of the tested substrates (Fig. 5). VvGT14a preferred geraniol and citronellol but also efficiently (greater than 80% relative activity) glucosylated nerol, hexanol, and octanol. Additionally, VvGT14a showed catalytic activity toward further monoterpenes (terpineol, 8-hydroxylinalool, and linalool), short-chain monoalcohols (3-methyl-2-butenol, 3-methyl-3-butenol, cis-3-hexenol, and trans-2-hexenol), benzyl alcohol, phenylethanol, eugenol, farnesol, mandelonitrile, and furaneol. The tested anthocyanidins and flavonoids (cyanidin, pelargonodin, quercetin, and kaempferol) were not converted at all (less than 1%). The three active proteins VvGT15a to VvGT15c showed a more limited substrate spectrum and glucosylated primarily geraniol, citronellol, nerol, octanol, and hexanol. VvGT15a and VvGT15c were also able to use 8-hydroxylinalool and trans-2-hexenol as acceptor molecules, and VvGT15a had low activity for farnesol. Other tested substrates were not converted. VvGT16 showed highest activity toward benzyl alcohol, geraniol, and hexanol (greater than 80% relative activity). Additionally, the protein transformed the terpenoids citronellol and nerol as well as phenylethanol, 3-methyl-2-butenol, trans-2-hexenol, and cis-3-hexenol. The formation of monoterpenyl glucosides was confirmed by HPLC-MS/MS analysis in comparison with chemically synthesized glucosides (Fig. 6). The retention times and fragmentation patterns of the reference material and products formed by VvGT14a, VvGT15a, and VvGT16 were identical and in accordance with the proposed fragmentation mechanism (Domon and Costello,

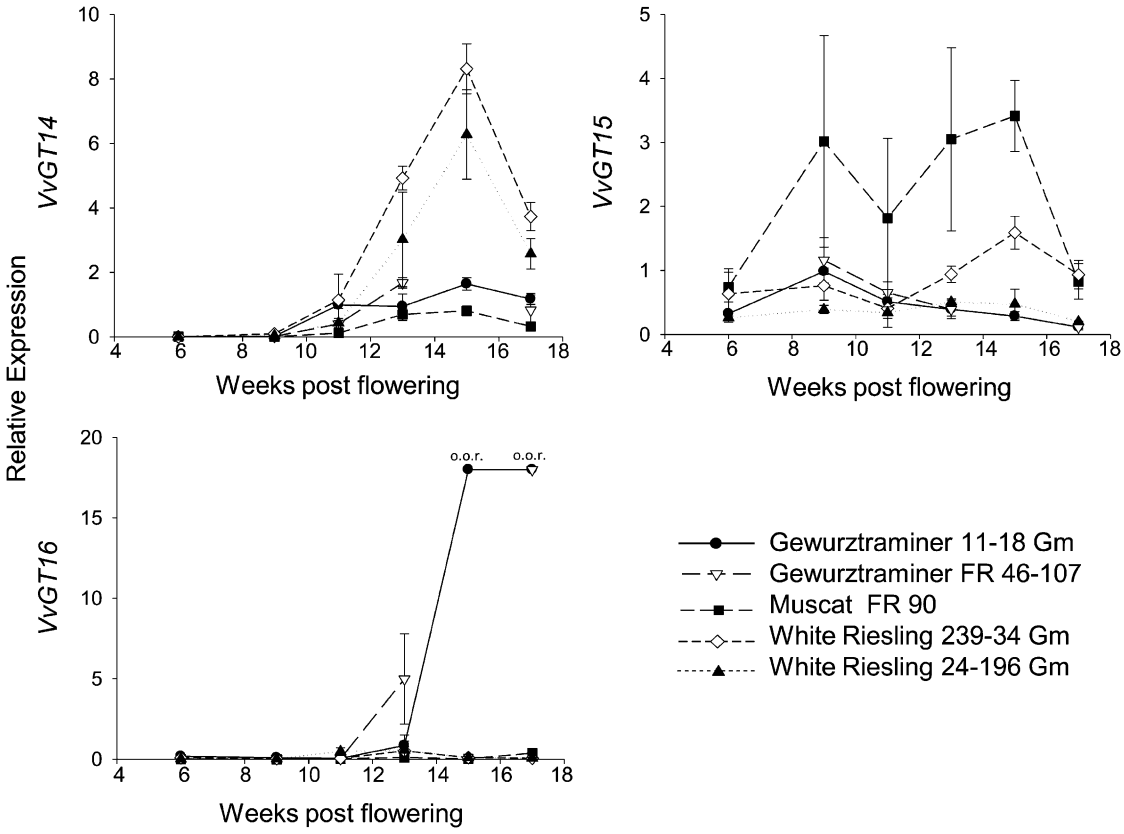

Figure 4. Gene expression analysis of *VvGTs* by GeXP. Different stages of berry development are given as weeks after flowering. Expression was determined in berry skins (exocarp) of five different cultivars and clones. Mean values ± SD of three independent experiments are shown. o.o.r., Out of range.

1988; Cole et al., 1989; Salles et al., 1991). Besides, selected glucosides of the transformed terpenoids were visualized by radio-thin-layer chromatography (TLC; Supplemental Figs. S7 and S8). The extracted radioactivity of the enzyme assays consisted exclusively of the terpenyl monoglucosides, except when 8-hydroxylinalool was used. It seemed that this monoterpene diol is glucosylated at both hydroxyl groups as two spots; presumably, the monoglucoside and diglucoside appeared on the radio-TLC plate. The two allelic enzymes VvGT14b and VvGT14c were unable to glycosylate any of the tested substrates. The alignment of the three VvGT14 alleles showed that VvGT14c has an internal deletion of 21 amino acids at position 165 (Supplemental Fig. S9), while VvGT14a and VvGT14b differed in a single position (P391L).

Enantioselectivity of VvGT14a, VvGT15a to VvGT15c, and VvGT16

Grape berries accumulate free and bound *S*-citronellol and *S*-linalool, albeit in lower levels than nerol and geraniol (Table I; Luan et al., 2004). To elucidate the enantiomeric preference of VvGT14a and VvGT15a, racemic citronellol was used as substrate and racemic linalool was transformed by VvGT14a. Chiral-phase GC-MS analysis of liberated citronellol after acid hydrolysis of citronellyl β-D-glucoside demonstrated no enantiomeric discrimination by VvGT14a and VvGT15a if the reaction mixture was incubated for a prolonged time (24 h; Fig. 7). Nevertheless, VvGT15a to VvGT15c and VvGT14a preferred *S*- over *R*-citronellol (1/0.4 and 1/0.8, respectively) when choosing short incubation times for kinetic assays (Supplemental Fig. S10, A and C), whereas VvGT16 transformed *R*- and *S*-citronellol with the same efficiency in radiochemical assays (Supplemental Fig. S10B). Accordingly, the kinetic data for VvGT15a to VvGT15c were calculated for *S*-citronellol (Table II). Furthermore, liberated linalool, after enzymatic hydrolysis of linaloyl β-D-glucoside (formed by VvGT14a), showed a slight enrichment of the *R*-enantiomer (Fig. 7). It is important to mention that the hydrolysis of racemic (1:1 diasteromeric mixture) linaloyl β-D-glucoside by AR 2000 revealed no enantiomeric discrimination by the action of this enzyme, which confirmed the results of previous works (Gunata et al., 1990; Lücker et al., 2001). Thus, VvGT14a and VvGT15a to VvGT15c show low enantioselectivity toward the *S*-enantiomer of citronellol and VvGT14a toward *R*-linalool during short-term assays.

Table I. *Amounts of free monoterpenes and monoterpenyl β-D-glucosides in grape skins during grape ripening*

Plant material was prepared and analyzed as described in "Materials and Methods." Grape berries were collected during grape ripening at the indicated weeks after flowering. n.d., Not detected; –, not determined. Amounts are listed in mg kg^{-1} grape skins ($n = 2$) and taken from Bönisch et al. (2014) and Supplemental Table S6.

Grape Cultivar	Product	Type	Weeks after Flowering					
			6	9	11	13	15	17
White Riesling 239-34 Gm	Linalool	Free	n.d.	n.d.	n.d.	n.d.	0.13 ± 0.18	n.d.
		β-D-Glucosides	n.d.	n.d.	n.d.	0.10 ± 0.08	0.17 ± 0.01	1.71 ± 0.54
	Nerol	Free	n.d.	n.d.	n.d.	n.d.	n.d.	n.d.
		β-D-Glucosides	n.d.	n.d.	n.d.	n.d.	n.d.	0.05 ± 0.03
	Geraniol	Free	n.d.	n.d.	0.09 ± 0.01	0.25 ± 0	0.26 ± 0.15	n.d.
		β-D-Glucosides	n.d.	n.d.	n.d.	n.d.	0.06 ± 0.02	0.14 ± 0.06
	Citronellol	Free	n.d.	n.d.	0.03 ± 0.01	0.05 ± 0.01	n.d.	n.d.
		β-D-Glucosides	n.d.	n.d.	n.d.	0.03 ± 0.02	n.d.	n.d.
White Riesling 24-196 Gm	Linalool	Free	n.d.	n.d.	n.d.	n.d.	0.11 ± 0	n.d.
		β-D-Glucosides	n.d.	n.d.	n.d.	0.07 ± 0.02	0.27 ± 0.02	0.61 ± 0.1
	Nerol	Free	n.d.	n.d.	n.d.	n.d.	0.08 ± 0	n.d.
		β-D-Glucosides	n.d.	n.d.	n.d.	n.d.	0.01 ± 0.01	n.d.
	Geraniol	Free	0.11 ± 0.03	0.06 ± 0	0.17 ± 0	0.24 ± 0.02	0.48 ± 0.01	0.67 ± 0.04
		β-D-Glucosides	n.d.	n.d.	n.d.	0.02 ± 0	0.07 ± 0.02	0.14 ± 0.02
	Citronellol	Free	0.05 ± 0	n.d.	n.d.	0.06 ± 0.02	0.09 ± 0.01	n.d.
		β-D-Glucosides	n.d.	n.d.	n.d.	n.d.	n.d.	n.d.
Gewurztraminer FR 46-107	Linalool	Free	–	n.d.	n.d.	n.d.	–	n.d.
		β-D-Glucosides	–	n.d.	n.d.	n.d.	–	n.d.
	Nerol	Free	–	n.d.	n.d.	n.d.	–	n.d.
		β-D-Glucosides	–	n.d.	n.d.	n.d.	–	0.01 ± 0.01
	Geraniol	Free	–	n.d.	0.11 ± 0.01	n.d.	–	0.20 ± 0.01
		β-D-Glucosides	–	0.02 ± 0.02	n.d.	0.01 ± 0.002	–	0.03 ± 0.04
	Citronellol	Free	–	n.d.	n.d.	n.d.	–	n.d.
		β-D-Glucosides	–	n.d.	n.d.	n.d.	–	n.d.
Gewurztraminer 11-18 Gm	Linalool	Free	n.d.	n.d.	n.d.	n.d.	n.d.	n.d.
		β-D-Glucosides	n.d.	0.1 ± 0.04	n.d.	n.d.	n.d.	n.d.
	Nerol	Free	n.d.	n.d.	0.13 ± 0.02	0.71 ± 0.04	1.25 ± 0.15	1.75 ± 0.05
		β-D-Glucosides	n.d.	n.d.	0.06 ± 0.01	0.23 ± 0.11	0.72 ± 0.22	0.87 ± 0.2
	Geraniol	Free	0.44 ± 0.06	0.88 ± 0.06	0.81 ± 0.07	2.62 ± 0.38	3.47 ± 0.66	5.26 ± 0.52
		β-D-Glucosides	0.08 ± 0	0.04 ± 0.01	0.18 ± 0.01	0.55 ± 0.16	1.72 ± 0.18	1.53 ± 0.4
	Citronellol	Free	0.12 ± 0.03	0.31 ± 0.01	0.27 ± 0.02	0.49 ± 0.01	0.48 ± 0.1	0.51 ± 0.02
		β-D-Glucosides	0.09 ± 0.01	0.08 ± 0.02	0.12 ± 0.01	0.21 ± 0.06	0.48 ± 0.02	0.29 ± 0.06
Muscat a petits grains blanc FR 90	Linalool	Free	0.06 ± 0.02	n.d.	n.d.	0.13 ± 0.02	3.03 ± 0.01	0.62 ± 0.12
		β-D-Glucosides	0.11 ± 0	0.12 ± 0.03	n.d.	0.05 ± 0.01	0.27 ± 0.10	0.37 ± 0.16
	Nerol	Free	n.d.	n.d.	0.16 ± 0.03	0.31 ± 0.04	0.78 ± 0.15	0.94 ± 0.05
		β-D-Glucosides	0.03 ± 0	0.04 ± 0.02	n.d.	0.09 ± 0.02	0.47 ± 0.05	0.57 ± 0.10
	Geraniol	Free	0.18 ± 0.04	0.53 ± 0.06	1.64 ± 0.62	1.00 ± 0.21	1.20 ± 0.21	1.21 ± 0.13
		β-D-Glucosides	0.03 ± 0	0.07 ± 0.03	0.05 ± 0.03	0.09 ± 0.02	0.45 ± 0.09	0.24 ± 0.08
	Citronellol	Free	0.09 ± 0.03	0.11 ± 0.01	0.20 ± 0.06	0.15 ± 0.01	0.21 ± 0	0.23 ± 0
		β-D-Glucosides	n.d.	0.07 ± 0.04	0.04 ± 0.02	0.04 ± 0.01	0.12 ± 0.05	n.d.

The enantiomers of racemic monoterpenes react with different reaction rates in the enzymatic reactions with VvGT14a and VvGT15a to VvGT15c.

Biochemical Characterization of VvGT14a, VvGT15a to VvGT15c, and VvGT16

The assay conditions were optimized for the conversion of geraniol to determine the kinetic constants of the active enzymes. The highest activity of VvGT14a, VvGT15a to VvGT15c, and VvGT16 was found in Tris-HCl buffer (pH 8.5, 7.5, and 8.5, respectively) at 30°C. The product formation of VvGT14a (0.2 μg of purified enzyme) was linear for at least 90 min. K_m and turnover number k_{cat} values were obtained for geraniol, citronellol, nerol, terpineol, 8-hydroxylinalool, and linalool with a constant UDP-Glc level (108 μM) and for UDP-Glc with a fixed geraniol concentration (100 μM; Table II). The

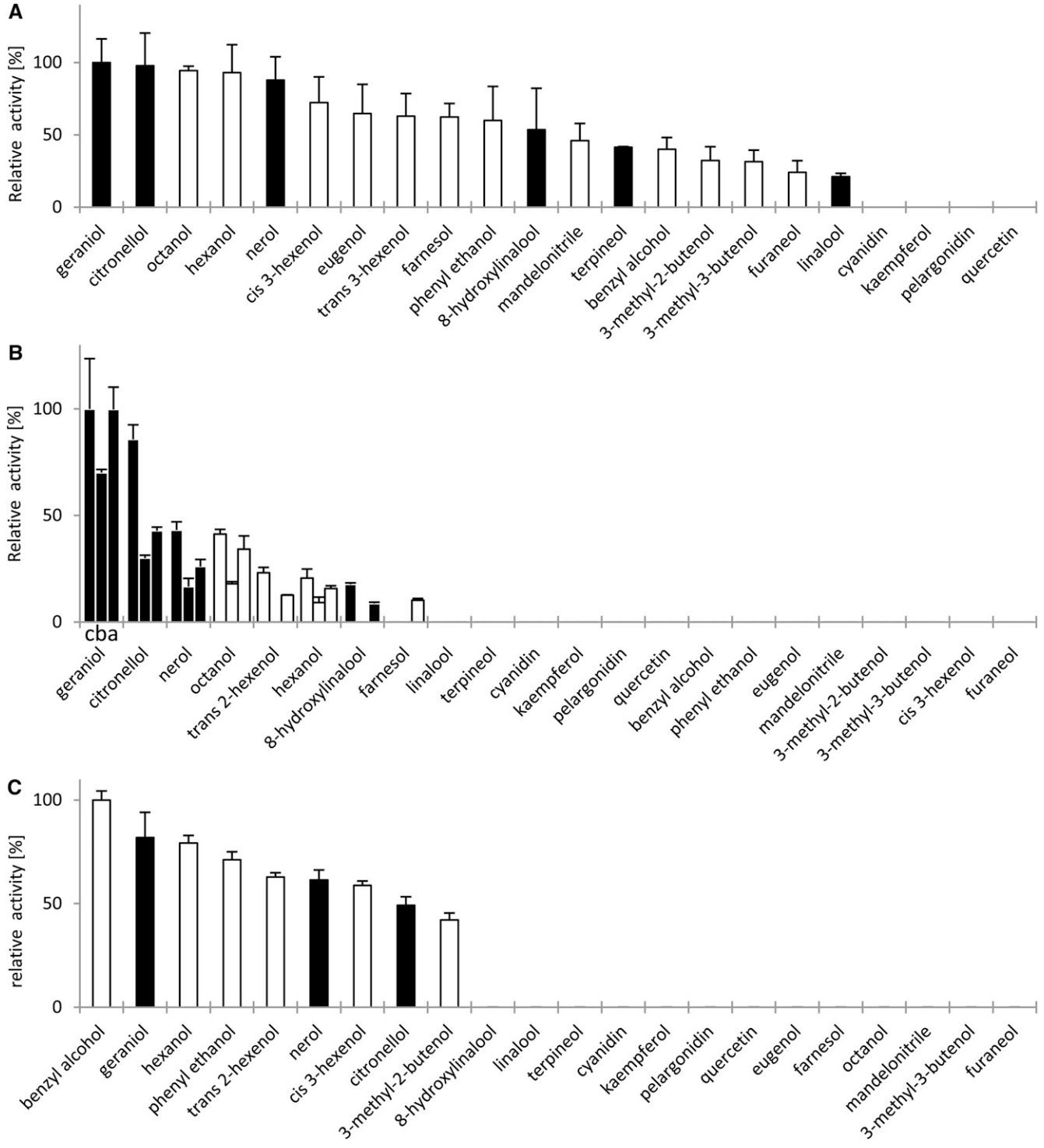

Figure 5. Relative specific activity (%) of VvGT14a (A), VvGT15a to VvGT15c (B), and VvGT16 (C) proteins from grape toward putative substrates as determined by radiochemical analysis with UDP-[^{14}C]Glc. Relative activities refer to the highest levels of extractable radioactivity that were measured for the conversion of geraniol (100%) in the case of VvGT14a and VvGT15a to VvGT15c (order of columns is 15c, 15b, and 15a) and benzyl alcohol (100%) in the case of VvGT16. Data for two biological and two technical replicates are shown. Black and white bars represent monoterpenoids and nonmonoterpenoids, respectively.

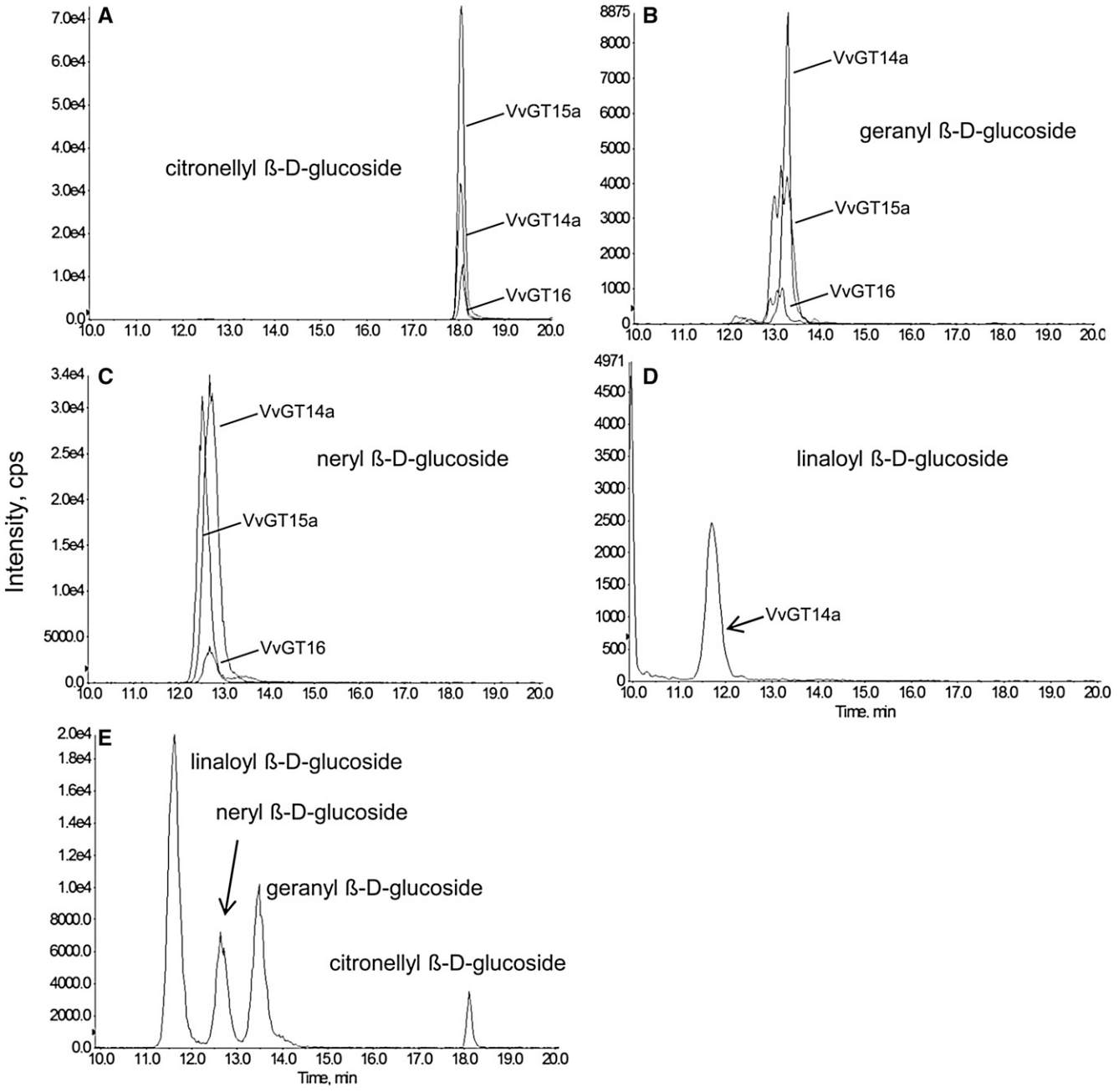

Figure 6. Detection of monoterpenyl β-D-glucosides as products of VvGT14a, VvGT15a, and VvGT16 by ESI-HPLC-MS/MS. HPLC-MS/MS analysis of citronellyl β-D-glucoside (A), geranyl β-D-glucoside (B), neryl β-D-glucoside (C), and linaloyl β-D-glucoside (D) formed by VvGT14a, VvGT15a, and VvGT16 and a mixture of synthesized monoterpenyl β-D-glucosides (E) is shown. Chromatograms display an overlay of single-product measurements, and traces show the total ion current of the characteristic transitions (see "Materials and Methods"). Gaussian smoothing was partly applied. The poor peak shapes of geranyl glucoside (B) and neryl glucoside (C) are probably caused by overloading of the chromatographic column.

kinetic parameters were determined from a hyperbolic Michaelis-Menten saturation curve. Due to the low conversion rates of 8-hydroxylinalool, terpineol, and linalool, the amount of purified enzyme was increased (2, 2, and 10 μg of protein, respectively). Interestingly, the K_m and k_{cat} values of VvGT14a for citronellol, geraniol, nerol, and UDP-Glc were quite similar (K_m, 9–10 μM; k_{cat}, 0.02 s^{-1}; k_{cat}/K_m, 2.0–2.6 s^{-1} mM^{-1}), while the kinetic data for 8-hydroxylinalool, terpineol, and linalool explained the significantly lower enzyme activity toward these substrates. The kinetic data of VvGT15a to VvGT15c (0.5 or 1 μg of purified enzyme) were maintained for geraniol, *S*-citronellol, nerol, and 8-hydroxylinalool with a fixed UDP-Glc amount (833 μM) and for UDP-Glc

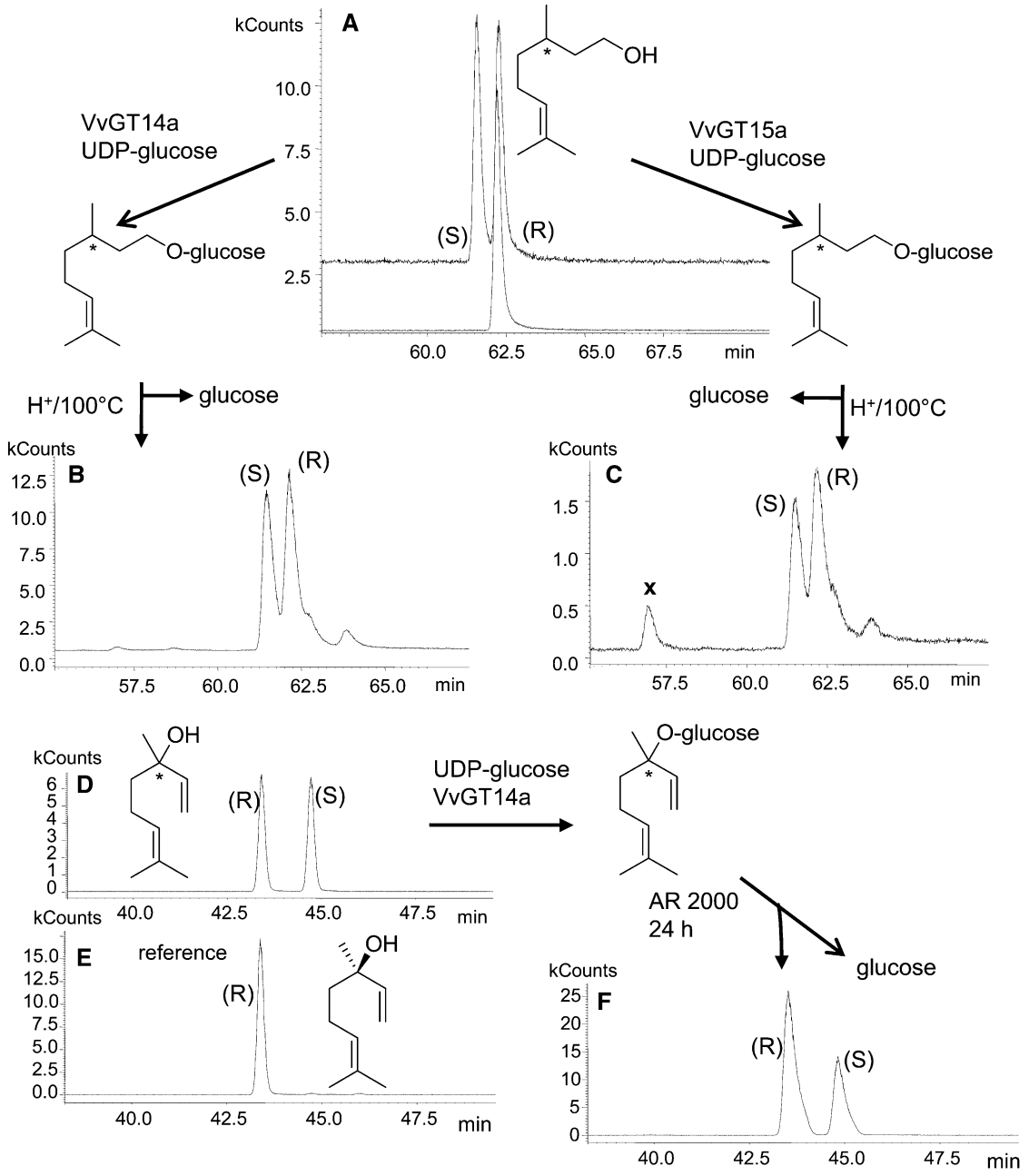

Figure 7. Enantioselectivity of VvGT14a and VvGT15a determined by chiral-phase SPME-GC-MS analysis of citronellol and linalool. A, A racemic mixture of *R,S*-citronellol was used as a substrate for VvGT14a and VvGT15a, and enantiomerically pure *R*-citronellol was used as a reference. B and C, Racemic citronellol is released by acid-catalyzed hydrolysis of citronellyl β-D-glucoside formed by VvGT14a and VvGT15a. Signals labeled with × are hydrolysis by-products. Chromatograms are shown in selected ion monitoring mode by using the characteristic ion traces *m/z* 69, 81, and 123 for citronellol. D, A racemic mixture of *R,S*-linalool was used as a substrate for VvGT14a. E, Enantiomerically pure *R*-linalool was used as reference material. F, A slight preference for *R*-linalool is revealed after enzymatic hydrolysis with AR 2000. Chromatograms are shown in selected ion monitoring mode (*m/z* 71 and 93).

with a constant geraniol concentration (1.25 mM; Table II). The formation of geranyl, neryl, and citronellyl β-D-glucoside was linear for at least 10 min (VvGT15c) and 20 min (VvGT15a and VvGT15b) but was extended for 8-hydroxylinaloyl β-D-glucoside up to 30 min (VvGT15c) and 60 min (VvGT15a and VvGT15b). The kinetic data confirmed the high enzymatic activity of the VvGT15 alleles toward geraniol and UDP-Glc. The K_m and k_{cat} values for *S*-citronellol and nerol were similar, whereas 8-hydroxylinalool was a poor substrate. Furthermore, the data illustrated that VGT15c is superior to VvGT15a and VvGT15b. The kinetics of VvGT16 were calculated

Table II. *Kinetics of VvGT14, VvGT15a to VvGT15c, and VvGT16*

Enzyme	Substrate	K_m	k_{cat}	k_{cat}/K_m
		μM	s^{-1}	$s^{-1}\ mM^{-1}$
VvGT14	Citronellol (racemic)	9 ± 0.3	0.02	2.5
	Geraniol	9 ± 1.2	0.02	2.6
	Nerol	10 ± 0.7	0.02	2.0
	8-Hydroxylinalool	48 ± 2.0	0.002	0.03
	Terpineol	33 ± 4.4	0.003	0.1
	Linalool (racemic)	47 ± 0.1	0.0003	0.01
	UDP-Glc	16 ± 0.03	0.03	1.6
VvGT15a	*S*-Citronellol	29 ± 3.0	0.02	0.9
	Geraniol	63 ± 2.4	0.12	1.9
	Nerol	48 ± 1.7	0.04	0.7
	8-Hydroxylinalool	32 ± 1.4	0.003	0.1
	UDP-Glc	49 ± 12.0	0.18	3.7
VvGT15b	*S*-Citronellol	55 ± 1.3	0.03	0.6
	Geraniol	81 ± 1.0	0.10	1.2
	Nerol	40 ± 3.7	0.03	0.8
	8-Hydroxylinalool	33 ± 1.8	0.003	0.1
	UDP-Glc	43 ± 1.0	0.17	4.1
VvGT15c	*S*-Citronellol	20 ± 1.6	0.03	1.8
	Geraniol	43 ± 0.7	0.17	3.9
	Nerol	28 ± 0.9	0.06	2.2
	8-Hydroxylinalool	17 ± 0.2	0.004	0.3
	UDP-Glc	51 ± 1.6	0.26	5.0
VvGT16	Citronellol (racemic)	108 ± 2.5	0.008	0.07
	Geraniol	355 ± 14	0.015	0.04
	Nerol	118 ± 4.7	0.009	0.08
	UDP-Glc	149 ± 10	0.013	0.09

for geraniol, citronellol, and nerol (Table II). The product formation of VvGT16 (5 μg of purified protein) was linear for at least 4 h. K_m and k_{cat} values were obtained for the monoterpenes with a constant UDP-Glc level (512.5 μM) and for UDP-Glc with a fixed geraniol concentration (1.25 mM). VvGT16 exhibited the lowest enzymatic activity toward the substrates of the tested UGTs.

Identification of the Natural Substrates of VvGT14a, VvGT15a to VvGT15c, and VvGT16

ABMP allows the unbiased discovery of enzymatic activities encoded by genes of unknown function. This approach applies chromatographic methods to analyze the effects of a recombinant enzyme on the homologous cellular extract as a physiologic library of potential substrates and products (de Carvalho et al., 2010; Duckworth and Aldrich, 2010). We adapted this method to reveal the natural substrates of VvGT14a, VvGT15a to VvGT15c, and VvGT16 (Fig. 8). In brief, glycosides were isolated by solid-phase extraction from grape skins (cv Gewurztraminer 11-18 Gm) and blooms ('Muscat'), as they showed the highest expression levels of the target genes. An aglycone library of the two tissues was obtained by enzymatic hydrolysis of the glycosides followed by liquid-liquid extraction of the released alcohols and acids. This physiologic library, which contained potential natural substrates of UGTs, was screened with recombinant VvGTs and either radiochemically labeled or unlabeled UDP-Glc. The formed glycosides were separated by TLC and visualized by radiodetection, whereas identification could be achieved by liquid chromatography-tandem mass spectrometry (LC-MS/MS) analysis and, after hydrolysis, by GC-MS and LC-MS (Fig. 8). Initially, the aglycone extracts were incubated with the purified recombinant enzymes (VvGT14a, VvGT15a, and VvGT16) using radiolabeled UDP-[^{14}C]Glc. Formed products were extracted; radioactivity was quantified by liquid scintillation counting (LSC) and analyzed by radio-TLC (Fig. 9). Screening of the aglycone library obtained from grape skins by VvGT14a and VvGT15a yielded products that showed identical chromatographic properties to geranyl β-D-glucoside. Enzymatic hydrolysis of the glucosides formed by VvGT14a liberated a substantial amount of geraniol but also remarkable quantities of citronellol, nerol, benzyl alcohol, phenylethanol, and linalool (Fig. 9). A similar result was gained with VvGT15a. VvGT16 did not form a visible product either by using the berry or from the bloom extracts. The extract from bloom was only tested with VvGT16. Thus, the aglycone library clearly enabled the detection and identification of the natural substrates of VvGT14a and VvGT15a and confirmed the role of these enzymes during grape berry ripening.

DISCUSSION

Small-molecule glycosyltransferases transfer carbohydrates to a wide range of acceptors, from antibiotics, lipids, hormones, and secondary metabolites to toxins and anthropogenic chemicals (Bowles et al., 2006). Recent progress in genome sequencing has allowed an assessment of the extent of the *UGT* multigene family in plants. UGT proteins can be easily identified by a signature motif in their primary sequence that is thought to be involved in the binding to the UDP moiety of the sugar nucleotide (Yonekura-Sakakibara and Hanada, 2011). Numerous in vitro studies have demonstrated that a single *UGT* gene product can glycosylate multiple structurally diverse substrates, whereas multiple UGTs can also glycosylate the same substrate. Thus, in cells, substrate availability can be a determining factor of the product spectrum, and redundancy points to sophisticated gene regulation mechanisms. Although the glycosylation of plant hormones, phenylpropanoids, flavonoids, betalains, and coumarins by recombinant UGTs has been described frequently, enzymatic transfer to monoterpenols has been observed quite rarely. Geraniol, nerol, and citronellol have been identified as promiscuous substrates of the cyanohydrin UGT from sorghum (*Sorghum bicolor*; Hansen et al., 2003) and were among the terpene alcohols that were glycosylated by a group of 27 UGTs from Arabidopsis (Caputi et al., 2008, 2010). A BLAST search for similar sequences in the grape genome yielded candidate genes that were analyzed in detail in our study, as it has been assumed that UGTs discriminate compounds as substrates in a lineage-specific

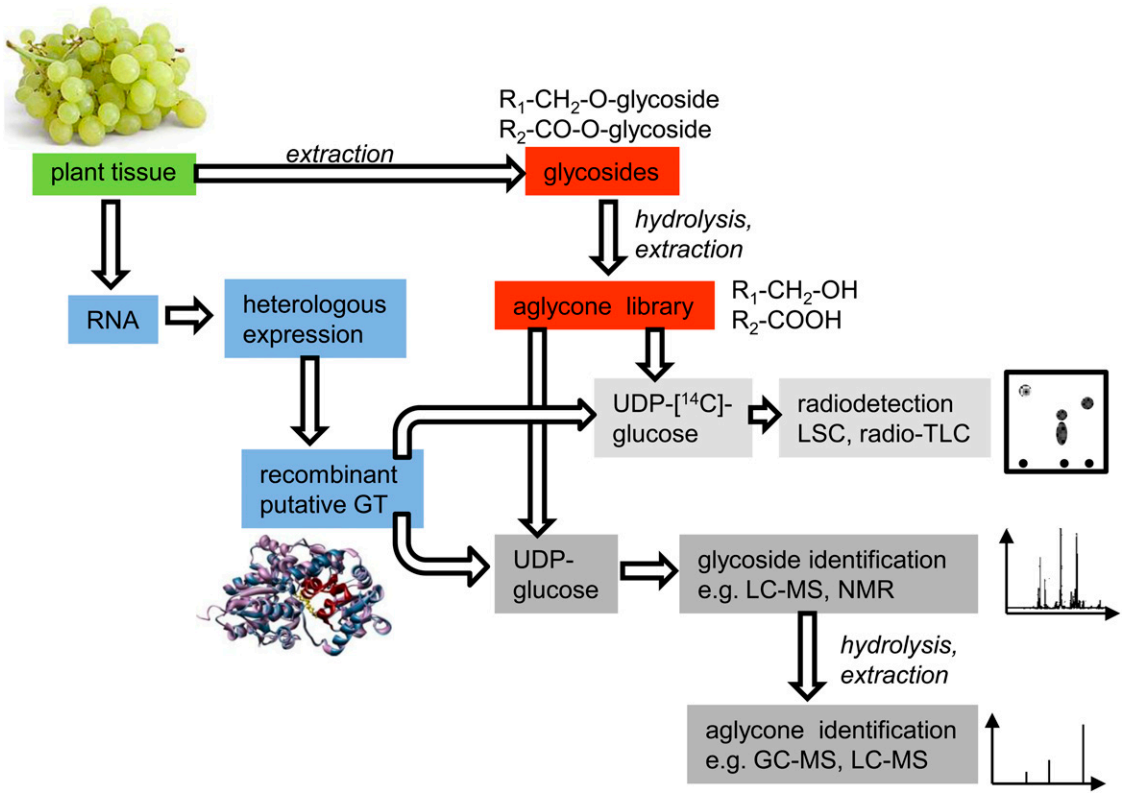

Figure 8. Targeted functional screening of small-molecule glucosyltransferases by means of aglycone libraries prepared from different plant tissues.

manner (Yonekura-Sakakibara and Hanada, 2011). Since enzymes involved in secondary metabolism display broad substrate tolerance (in this context, tolerance describes the property of the enzyme much better than specificity, as specificity relates to a very limited number of substrates), forward and reverse genetic approaches are frequently applied to reveal in planta functions of genes. However, in nonmodel plants such as grape, these techniques are not yet very well established. Thus, alternative methods are needed. In this study, we propose a novel approach employing a physiologic library of aglycones to identify the natural substrates and function of UGTs by ABMP.

Correlation of Metabolite Analysis and Expression Analysis of Putative VvGTs

Only a few odor-impact compounds have been identified in wines. Among these are terpenes that significantly contribute to the floral and fruity characters to white wines (Marais, 1983). It has been suggested that monoterpene biosynthesis occurs during grape ripening, starting from berry set (Wilson et al., 1984), whereas our results revealed a large cultivar-based variation in the content of terpenes and their glycosidic derivatives (Table I). 'Gewurztraminer 11-18 Gm' and 'Muscat', two genotypes that are rich in monoterpenes, also accumulated high levels of the glucosides that can also be detected at early stages of berry set (6 weeks after flowering). Besides, the ratio of free to glycosylated terpenes differed for the cultivars and sampling dates, indicating differential glycosylation activities during berry ripening in the diverse genotypes. As terpenoids and their glucosides were accumulating in berry skins after veraison, the strong expression of *VvGT14*, *VvGT15*, and *VvGT16* during late stages of berry ripening suggested an important role during this period and led to in-depth analysis of these genes (Fig. 4). Notably, *VvGT14* transcript levels detected in both 'White Riesling' clones correlated well with the late formation of monoterpenyl glucosides in the same cultivars (Table I; Fig. 4), whereas the expression level of *VvGT15* in 'Muscat' showed a similar time-course pattern to the amounts of the glucosides. In 'Muscat', the transcription of *VvGT15* and the production of terpenyl glucosides started already at 6 to 9 weeks after flowering and remained at a high level. Besides, in 'Gewurztraminer 11-18 Gm', *VvGT15* expression peaked at 9 weeks after flowering and then decreased continuously, although monoterpenol derivatives accumulated to high levels in grape skin. However, compensation of VvGT15 activity by VvGT16 was assumed, as *VvGT16* expression levels even exceeded the range of GeXP quantification at the late stages of ripening. Based on the positive correlation of monoterpenyl glucoside evolution and transcript analysis, *VvGT14*, *VvGT15*, and *VvGT16* were chosen for further analysis.

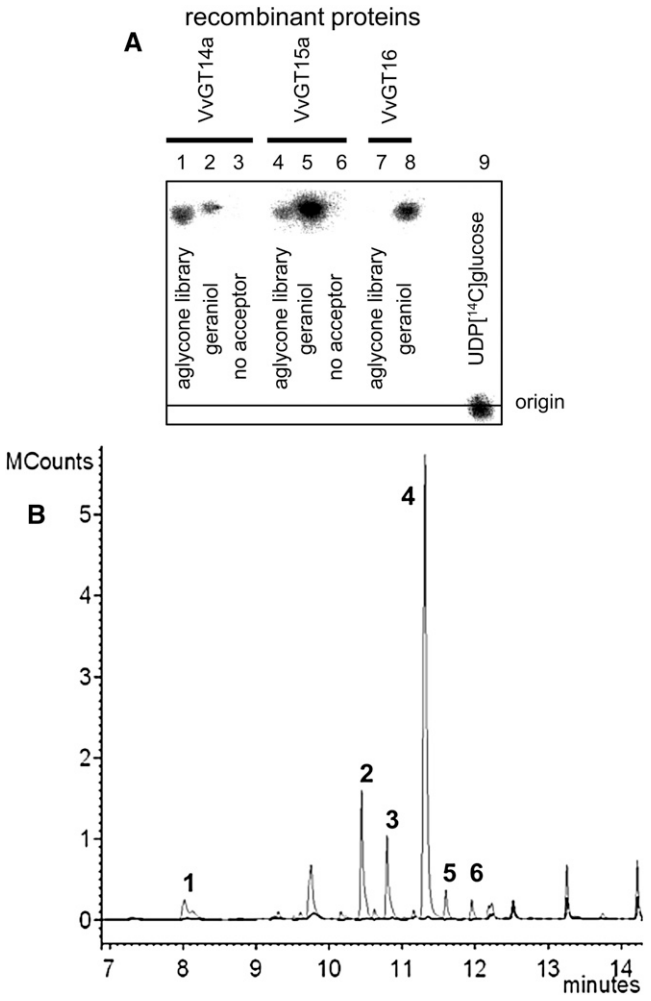

Figure 9. Functional screening of VvGT14a, VvGT15a, and VvGT16. A, Radio-TLC analysis of products formed by VvGT14a (lanes 1–3), VvGT15a (lanes 4–6), and VvGT16 (lanes 7–9) after incubation with the aglycone library obtained from grape berries of 'Gewurztraminer 11-18 Gm' (lanes 1, 4, and 7). Positive control was geraniol (lanes 2, 5, and 8) and negative control was no acceptor molecule (lanes 3 and 6); UDP [^{14}C] Glc (lane 9) was approximately 3,000 dpm. The plates were analyzed by digital autoradiography. The products formed from citronellol, geraniol, and nerol were verified by LC-MS analysis. B, GC-MS analysis (total ion chromatogram) of volatiles that were enzymatically released from glucosides that were formed by incubation of an aglycone library obtained from grape berries of 'Gewurztraminer 11-18 Gm' with UDP-Glc and VvGT14 (gray) or heat-inactivated VvGT14a (black) as a control. Peaks are as follows: 1, linalool; 2, citronellol; 3, nerol; 4, geraniol; 5, benzyl alcohol; and 6, phenylethanol. For response factors of volatiles (0.52–1.90) toward geraniol, see Supplemental Table S4. Thus, even when response factors are taken into account, geraniol is the major product that is released.

Biochemical Characterization of VvGT14a to VvGT14c, VvGT15a to VvGT15c, and VvGT16

One of three allelic forms of VvGT14 catalyzed the transfer of Glc to alcohols that have been shown to be glycosylated in grape skins (Wirth et al., 2001). Two alleles (b and c) were inactive. VvGT14a converted a broad range of tested substrates, among them monoterpenoids and short-chain aliphatic and aromatic alcohols, while flavonoids were not converted. Until now, only flavonoid and (hydroxyl)cinnamic acid glycosyltransferases have been characterized in grape (Offen et al., 2006; Jánváry et al., 2009; Ono et al., 2010; Khater et al., 2012). The K_m and k_{cat} values of VvGT14a for geraniol (9 μM and 0.02 s^{-1}), citronellol (9 μM and 0.02 s^{-1}), nerol (10 μM and 0.02 s^{-1}), and UDP-Glc (16 μM and 0.03 s^{-1}) were alike (Table II) and resembled the kinetic data of VvGT1 (Offen et al., 2006) and CaUGT2 (*Catharanthus roseus*; Masada et al., 2007) for their natural substrates quercetin (31 μM and 0.075 s^{-1}) and curcumin (43.9 μM and 0.0165 s^{-1}), respectively. The data were also similar to those of VvGT5 (5.6 μM and 7.16 s^{-1}), VvGT6 (9.24 μM and 0.76), and UGT71G1 (57 μM and 0.0175 s^{-1}) from *Medicago truncatula* (He et al., 2006) for the conversion of quercetin (Ono et al., 2010). Hence, the specificity constants (k_{cat}/K_m) identified the monoterpenol as the most probable in vivo substrate of VvGT14a. However, the K_m for terpineol, 8-hydroxylinalool, and linalool was 3- to 5-fold higher, while the turnover numbers were 10- to 100-fold lower than for geraniol, nerol, and citronellol. Thus, the enzyme efficiency values made it unlikely that they are converted by VvGT14a in planta.

The sequence comparison of the active VvGT14a allele with the two inactive alleles showed one point mutation at position 391 (P391L) in VvGT14b and a deletion of 21 amino acids at position 165 in VvGT14c, rendering them inactive (Supplemental Fig. S9). Pro in position 391 is located in the PSPG motif (for plant secondary product glycosyltransferase; Hughes and Hughes, 1994) and is quite conserved among UGTs (Osmani et al., 2009). The exchange of Pro to Leu in VvGT14b leads to an inactive enzyme and has not been reported yet.

The allelic forms of VvGT15a to VvGT15c showed a similar substrate spectrum (Fig. 5). Remarkably, these alleles had a distinct preference for the monoterpenes geraniol, citronellol, and nerol, as comparison with the accepted substrates of VvGT14a clearly demonstrated. The kinetics identified geraniol as the superior substrate (Table II). The turnover numbers of VvGT15a to VvGT15c for the glucosylation activity of geraniol (0.12, 0.1, and 0.17 s^{-1}, respectively) were 3- to 6-fold higher and the Michaelis-Menten constants (63, 81, and 43 μM, respectively), about 2-fold greater than the k_{cat} and K_m values for nerol and *S*-citronellol. This resulted in the highest enzyme specificity constant of VvGT15a to VvGT15c for geraniol and confirmed the data of the substrate screening (Fig. 5), whereas allele c was the most effective (k_{cat}/K_m = 3.9 s^{-1} mM^{-1}). All three alleles showed a 30- to 40- fold lower turnover number for 8-hydroxylinalool compared with geraniol, although the K_m value was similar to the ones obtained for *S*-citronellol and nerol.

Notably, the glucosylation of monoterpenols by UGT85B1, a cyanohydrin (mandelonitrile) glucosyltransferase from sorghum can be seen as promiscuous activity (Hansen et al., 2003). However, the K_m data of VvGT14a and VvGT15a to VvGT15c were 1.6- to 125-fold lower

and the k_{cat}/K_m values were up to 78 times higher than the data obtained for the glucosylation of terpenoids by UGT85B1. Mandelonitrile was only a poor substrate of VvGT14a and was not accepted at all by VvGT15a to VvGT15c.

VvGT16 glucosylated monoterpenols and some short-chain and aromatic alcohols, albeit with low efficiency (Fig. 5; Table II). Interestingly, benzyl alcohol, an alcohol that has been frequently detected in hydrolysates of glycosides from grape, showed the highest relative activity (Gunata et al., 1988). However, the low k_{cat}/K_m values argue against a role of VvGT16 in the glucosylation of these compounds in planta.

In Planta Substrates of VvGT14a and VvGT15a to VvGT15c

More than 200 volatiles have been identified in grape berries, and most of them are glycosylated (Sefton et al., 1996). Furthermore, about 240 putative *UGT* genes have been annotated in the genus *Vitis* genome (Jaillon et al., 2007). Since substrate promiscuity is a frequently observed feature of UGTs, unambiguous identification of their in vivo substrates becomes a challenge. Screening of VvGT14a, VvGT15a to VvGT15c, and VvGT16 with a number of alcohols that have been shown to be glycosylated in grape revealed broad substrate tolerance also for the UGTs isolated from grape. However, the clear correlation of spatial and temporal transcript accumulation of *VvGT14* and *VvGT15* in the 'White Riesling' clones and 'Muscat', respectively, with monoterpenyl glucoside evolution provided, to our knowledge, the first evidence for the biological function of the encoded proteins. Detailed biochemical analyses and structural confirmation of the products by LC-MS analysis further substantiated the hypothesis of the identification of the first monoterpenyl glucosyltransferases from grape.

However, ultimate proof was delivered by the application of ABMP of a physiologic aglycone library (Fig. 8), which has several advantages. An aglycone library can be prepared from any tissue that shows high *UGT* transcript levels. The library contains the natural substrates in high concentration, as they are enriched during the preparation of the extract and can be easily screened with recombinant UGT enzymes and various labeled and unlabeled UDP-sugars. The formation of products can be rapidly quantified by LSC and confirmed by TLC (Fig. 8). The identification of glycosides by LC-MS and NMR analyses is greatly facilitated, as levels of impurities are very low. Finally, the structure of the carbohydrate moiety is already known from the used UDP-sugar. VvGT14a and VvGT15a to VvGT15c readily formed radiolabeled products when incubated with an aglycone library obtained from grape skins of 'Gewurztraminer 11-18 Gm' (Fig. 9A). Geranyl and minor amounts of citronellyl and neryl glucoside (as their free alcohols after hydrolysis) were identified as products of VvGT14a and VvGT15a to VvGT15c (Fig. 9B). In contrast, VvGT16 did not form a glucosylated product, although the expression level of *VvGT16* and the amounts of monoterpenyl glucosides were extraordinarily high in berry skins in the late stages of ripening and blooms (cv Gewurztraminer 11-18 Gm). However, additional UDP-sugars, besides UDP-Glc, were not tested as putative donor molecules, and the possible formation of diglycosides and triglycosides of one aglycone was not taken into account (Gunata et al., 1988; Voirin et al., 1990; Jánváry et al., 2009). We conclude that by using alternative UDP-sugars for the screening of the libraries, novel glycosides can be formed and identified that also occur in nature. In addition, the combination of different UDP-sugars with a diversity of recombinant UGTs would also yield aglycones attached to diglycosides and triglycosides. Last but not least, the method can be applied in high-throughput screens. However, the insufficient release of aglycones by acidic and enzymatic hydrolysis and the instability of liberated aglycones are two drawbacks that have to be kept in mind. Moreover, the obtained glycosodic extract, which is used for ABMP, contains glycosides from various cellular compartments, like cytosol and vacuole. Because it is known that glycosyltranferases are usually located in the cytosol, it cannot be ruled out that, in an in vivo scenario, some aglycones and glycosyltransferases do not come into contact in intact cells. Nevertheless, ABMP of aglycone libraries has great potential to unravel the physiologic substrates of a wide range of UGTs and thus to clarify their biological roles.

Interestingly, VvGT14a and VvGT15a to VvGT15c also displayed high levels of activity toward aliphatic alcohols such as octanol, hexanol, and hexenols (Fig. 5). Grape leaves and berries contain appreciable amounts of glycosides derived from these alcohols (Wirth et al., 2001). However, functional screening of an aglycone library produced from glycosides isolated from grape exocarp did not reveal the aliphatic alcohols as natural substrates (Fig. 9), probably due to their low levels in this tissue. The amounts of glycoconjugates derived from aliphatic alcohols are much higher in leaves from grape cultivars (Wirth et al., 2001). Thus, we assume that VvGT14a and VvGT15a to VvGT15c might contribute, at least to a certain extent, to the formation of hexyl, hexenyl, and octyl glucoside in leaves. This hypothesis will be tested in future studies by functional screening of an aglycone library produced from leaves of grape.

Enantiomeric Discrimination

Free and glycosylated citronellol and linalool occur predominantly in the *S*-configuration in grape, whereas their free and glycosylated forms exhibit similar enantiomeric excesses (Luan et al., 2005). While VvGT14a and VvGT15a to VvGT15c preferentially glucosylated *S*-citronellol in short time assays, the enantioselectivity of these enzymes for citronellol was not observed in long-term studies (Fig. 7; Supplemental Fig. S10). This effect is characteristic for studies on the kinetic resolution of racemates (Strauss et al., 1999). The reaction

slows down at 50% conversion, when the fast-reacting enantiomer is almost consumed and only the slow-reacting counterpart is gradually transformed. Thus, the enantiomeric excess of the product peaks at 50% transformation and then decreases slowly but steadily. In contrast, VvGT14a preferred *R*- over *S*-linalool even in long-term assays. The slight preference for *R*-linalool explained the previously observed enrichment of this enantiomer in the glycosidically bound fraction of linalool in 'Morio Muskat' and 'Muscat Ottonel' berries relative to the free fraction (Luan et al., 2004). Hence, the moderate enantioselectivities of VvGT14a and VvGT15a to VvGT15c were in accordance with their proposed biological role, as the availability of highly enriched *S*-citronellol and *S*-linalool mainly determined the diastereomeric ratio of the glucosidic product.

CONCLUSION

In plants, UGTs represent a large gene family, whereas the individual gene products show substrate promiscuity, especially if they are related to secondary metabolism. In this study, we devised an ABMP method for targeted functional screening of small-molecule UGTs that allowed the rapid identification of in vivo substrates by using aglycone libraries prepared from different tissues. This approach has the potential to be broadly applied, as it is suitable for high-throughput screens.

ABMP of an aglycone library obtained from grape berry led to the identification of two glucosyltransferase genes that are involved in the metabolism of monoterpenols in vivo. Spatial and temporal gene expression analysis in combination with metabolite and chiral-phase analyses revealed that enzyme specificity and substrate availability dictate the formation of monoterpene glucosides during grape ripening. Furthermore, it appears that different UGTs such as VvGT14 and VvGT15a to VvGT15c are major players for monoterpenyl glucoside formation in different cultivars such as 'White Riesling' clones and 'Muscat', respectively.

MATERIALS AND METHODS

Plant Material

Grape (*Vitis vinifera*) vines of cv Gewurztraminer 11-18 Gm, Gewurztraminer FR 46-107, White Riesling 239-34 Gm, White Riesling 24-196 Gm, and Muscat a petit grains blanc FR 90 were grown in the Geisenheim research center vineyard in Geisenheim, Germany, during vintages 2011 and 2012. Grape berries, leaves, inflorescences, and roots were collected. Sampling was conducted for a total of six dates between 6 and 17 weeks after bloom in 2011, including berries from pea size to harvest ripeness. 'Muscat' FR 90 was additionally sampled in 2012 every 2 weeks from week 4 to week 18 after bloom (Fig. 1). After veraison (the onset of ripening), 100 berries were collected for the determination of ripening-related parameters like sugar content. For terpenoid analysis, 250 g of berries was stored at −20°C, while three replicates consisting of 10 berries were peeled and the skins immediately frozen in liquid nitrogen for subsequent RNA extraction. Roots were obtained from scions of 'White Riesling 239-34 Gm' and 'Gewurztraminer 11-18 Gm' grown in the greenhouse. Leaves were sampled from the same cultivars at the approximate ages of 1, 3, and 5 weeks. In addition, inflorescences at 4 and 2 weeks before flowering and at full bloom were collected in 2012. Samples were immediately frozen in liquid nitrogen and stored at −20°C until workup. Samples were extracted within 6 months of storage at −20°C.

Chemicals

Except where stated otherwise, all chemicals, solvents, and reference compounds were purchased from Sigma-Aldrich, Fluka, and Roth. UDP-[^{14}C]Glc (300 mCi mmol^{-1}, 0.1 mCi mL^{-1}) was obtained from American Radiolabeled Compounds. (*R*,*S*)-3,7-Dimethyl-1,6-octadien-3-ol (linalool) and (*E*)-3,7-dimethyl-2,6-octadien-1-ol (geraniol) were obtained from Roth. (*R*,*S*)-3,7-Dimethyl-6-octen-1-ol (citronellol) and pure (*R*)-(+)-β-citronellol were purchased from Sigma-Aldrich. (*Z*)-3,7-Dimethyl-2,6-octadien-1-ol (nerol) was purchased from Alfa Aesar. (*R*,*S*)-3,7-Dimethyl-6-octenyl β-D-glucopyranoside (citronellyl β-D-glucoside), (*Z*)-3,7-dimethyl-2,6-octadienyl β-D-glucopyranoside (neryl β-D-glucoside), and (*E*)-3,7-dimethyl-2,6-octadienyl β-D-glucopyranoside (geranyl β-D-glucoside) were synthesized according to the Koenigs-Knorr procedure (Paulsen et al., 1985). (*R*,*S*)-3,7-Dimethyl-1,6-octadienyl β-D-glucopyranoside (linaloyl β-D-glucoside), as a less reactive tertiary alcohol, was synthesized according to a modified Koenigs-Knorr procedure using another catalyst (Hattori et al., 2004). Deuterium-labeled 1,1-[^{2}H$_2$]citronellyl β-D-glucoside was prepared as described (Hill et al., 1994; Wüst et al., 1998). Spectral data of the synthesized compounds were in all cases in good agreement with the data given (Paulsen et al., 1985; Salles et al., 1991; Konda et al., 1997).

Sample Preparation for Metabolite Analysis

Grape berries were peeled, and 10 g (fresh weight) of the grape skins was taken for one analysis. In the case of root, leaf, and inflorescence, 4 g of plant material was taken per analysis. The material was frozen in liquid nitrogen, ground, and extracted with a mixture of phosphate buffer (0.1 M, pH 7) and 13% (v/v) ethanol for 24 h under nitrogen with exclusion of light (Jesús Ibarz et al., 2006). 2-Octanol was used as an internal standard for the determination of free monoterpenes. For the determination of monoterpenyl β-D-glucosides, stable isotope dilution analysis was applied, using [^{2}H$_2$]citronellyl β-D-glucoside as a labeled internal standard. The concentration of the internal standards was adapted for the cultivar, the tissue, and the ripening stage of the plant material. 2-Octanol was added in a range of 0.3 to 6.8 mg kg^{-1} plant material and [^{2}H$_2$]citronellyl-β-D-glucoside in a range of 0.1 to 3.5 mg kg^{-1} plant material. To purify the sample, Carrez reagents (Merck Millipore) were added (1 mL each), and the sample was then centrifuged at 14,500 rpm for 20 min at 5°C. The supernatant was taken for subsequent solid-phase extraction to isolate and separate free monoterpenes from glycosidically bound monoterpenes. Therefore, a 200-mg Lichrolut EN column (Merck) was conditioned as described (Piñeiro et al., 2004). Free monoterpenols were eluted with dichloromethane and glycosidically bound monoterpenols with methanol. For GC-MS detection, the dichloromethane fractions were dried with Na_2SO_4, concentrated using nitrogen to 200 μL, and analyzed. For HPLC-MS/MS detection, the methanolic fractions were concentrated under reduced pressure, and the residues were dissolved in water:acetonitrile (7:3, v/v). The samples were analyzed by LC-MS/MS.

Nucleic Acid Extraction

For total RNA extraction, plant material was ground to a fine powder in liquid nitrogen using mortar and pestle. One gram of the powder was used for RNA extraction with the cetyl-trimethyl-ammonium bromide method following an established protocol (Zeng and Yang, 2002) that was adapted by Reid et al. (2006) to meet the requirements of different grape tissues. The remaining genomic DNA was digested by DNase I and cleaned up with the High Pure RNA Isolation kit (Roche).

Transcription Analysis

Transcription analysis was performed using the GenomeLab GeXP Genetic Analysis System (Beckman Coulter), a multiplex quantitative gene expression analysis system. The gene expression patterns of eight VvGT genes and five reference genes (*VvActin* [*Vitis vinifera* gene of the globular multi-functional protein actin], *VvAP47* [*Vitis vinifera aspartic protease47* gene], *VvPP2A* [*Vitis vinifera protein phosphatase 2A*], *VvSAND*, [the gene was named *SAND*, as its location is next to the plasminogen related growth factor receptor *PRGFR*, which is thought to be the orthologue of *SEA* [EMBL : AJ010317], and *VvTIP41* [*Vitis vinifera TAP41-interacting protein*]) were analyzed simultaneously from

one sample of total RNA. Reverse transcription was carried out with the GenomeLab GeXP Start kit (Beckman Coulter) following the manufacturer's instructions. As an internal control gene, Kanamycin-resistance gene RNA was coreverse transcribed and subsequently amplified together with the reference genes and genes of interest. The gene-specific primers for reverse transcription are chimeric, providing a 19-nucleotide universal tag for the binding of universal reverse primers in the subsequent PCR. The final concentration of the primers ranged from 0.1 to 100 nM to compensate for the different transcription levels of the analyzed genes (Supplemental Table S1). Multiplex PCRs were conducted with Thermo-Start DNA Polymerase (Thermo Fisher Scientific). Each reaction contained 9.3 μL of reverse transcription products as template and 10.7 μL of a PCR mix including gene-specific forward primers, providing an 18-nucleotide universal tag (Supplemental Table S1). The universal forward primer is labeled with a fluorescent dye for detection during subsequent capillary electrophoresis. Primer pairs were designed to yield PCR products ranging from 119 to 374 bp and differing in size by at least 8 bp. Of each PCR product, 4 μL was separated by capillary electrophoresis using the GenomeLab Genetic Analysis System (Beckman Coulter). Individual standard curves for each gene in the multiplex were determined with serial 2-fold dilutions ranging from 3.91 to 500 ng of an RNA mixture from all samples. Raw data were analyzed using the Fragment Analysis tool. The fragment data of the standard curves and samples were then normalized to the peak area of Kanamycin-resistance gene RNA with the Express Analysis tool. Subsequently, the relative signal level of each sample replicate was interpolated from the standard curve. The data were further normalized to the geometric mean of the five reference genes with the Quant tool. All software for GeXP data analysis was purchased from Beckman Coulter.

Comparative Sequencing

The reference genome of PN40024 (Jaillon et al., 2007) was used to design gene-specific primers in the untranslated regions of the three putative VvGT genes, *VvGT14*, *VvGT15*, and *VvGT16*, using the tool Primer-BLAST (Ye et al., 2012). Primers were purchased from Eurofins MWG Operon (Supplemental Table S2). Complementary DNA (cDNA) synthesis was performed with the SuperScript III First-Strand Synthesis SuperMix (Life Technologies) following the manufacturer's instructions. The template for cDNA synthesis was total RNA, extracted from samples with high transcript levels of the concerned VvGT gene, as determined by gene expression analysis. The cDNA was used as a template in the following PCR. PCR was performed with Phusion DNA Polymerase (Thermo Fisher Scientific) using high-fidelity buffer and the following thermal cycling conditions: 98°C for 30 s, followed by 32 cycles consisting of 98°C for 5 s, 60°C for 5 s, and 72°C for 30 s, and a final elongation step of 72°C for 1 min. PCR products were gel purified with the Wizard SV Gel and PCR Clean-Up System (Promega). A-tailing of purified PCR products was performed with *Taq* DNA Polymerase (Thermo Fisher Scientific). A-tailed PCR products were ligated into pGEM-T Easy vector (Promega) and cloned in One Shot TOP10 Chemically Competent *Escherichia coli* (Life Technologies). Plasmids were isolated with the PureYield Plasmid Miniprep System (Promega) and sequenced with the vector-specific primers M13 uni (−21) and M13 rev (−29) on an ABI 3730 capillary sequencer (StarSEQ). Raw data were edited with FinchTV software (Geospiza). Sequences were assembled with SeqMan and aligned with MegAlign (DNASTAR).

Construction of Expression Plasmids

The full-length open reading frames of the VvGT sequences were subcloned into the pGEM-T Easy vector (Promega). All genes were amplified with primers introducing *Bam*HI und *Not*I restriction sites. Subsequently, the genes were cloned in frame with the N-terminal GST tag into the pGEX-4T-1 expression vector (Amersham Bioscience). Gene identity was confirmed by sequencing (Eurofins MWG Operon).

Heterologous Protein Expression

Recombinant protein was expressed in *E. coli* BL21 (DE3) pLysS (Novagen). Precultures were grown overnight at 37°C in Luria-Bertani medium containing 100 μg mL^{-1} ampicillin and 23 μg mL^{-1} chloramphenicol. The next day, 1 L of Luria-Bertani solution containing the appropriate antibiotics was inoculated with 50 mL of the preculture. The culture was grown at 37°C at 160 rpm until the optical density at 600 nm reached 0.6 to 0.8. After cooling the culture to 16°C, 1 mM isopropylthio-β-galactoside was added to induce protein expression. Cultures were incubated overnight at 16°C to 18°C at 160 rpm. Cells were harvested by centrifugation and stored at −80°C. Negative controls were carried out with *E. coli* BL21 (DE3) pLysS cells containing the empty expression vector pGEX-4T-1.

Cell Lysis and Purification

Recombinant GST fusion proteins were purified by GST Bind resin (Novagen) following the manufacturer's instructions. Briefly, the cells were resuspended in the binding buffer containing 10 mM 2-mercaptoethanol. Cells were disrupted by sonication. The crude protein extract was incubated for 2 h with the GST Bind resin to bind GST fusion protein. The recombinant protein was eluted with GST elution buffer containing reduced glutathione and quantified by Bradford solution (Sigma-Aldrich). The presence of the expressed proteins was confirmed by SDS-PAGE and western blot using anti-GST antibody.

Activity Assay and Kinetics

In the initial screening, each reaction mixture (200 μL in total) contained Tris-HCl buffer (100 mM, pH 8, with 10 mM 2-mercaptoethanol), 37 pmol of UDP-[^{14}C]Glc (0.01 μCi; Biotrend), substrate (50 μL of a 1 mg mL^{-1} stock solution), and purified protein (0.5–0.8 μg μL^{-1}). The reaction mixture was incubated at 30°C for 18.5 h. The assays were stopped by adding 1 μL of 24% (v/v) TCA and extracted with 500 μL of water-saturated 1-butanol. The organic phase was mixed with 2 mL of Pro Flow P+ cocktail (Meridian Biotechnologies), and radioactivity was determined by LSC (Tri-Carb 2800TR; PerkinElmer). Additionally, negative controls without substrate were performed. After determining the optimal conditions for the best substrate of each gene, the substrate screening was repeated under these conditions. The kinetic data were determined with increasing concentrations of the substrates (VvGT14a, citronellol, geraniol, 8-hydroxylinalool, linalool, nerol, and terpineol; VvGT15a to VvGT15c, *S*-citronellol, geraniol, 8-hydroxylinalool, and nerol; VvGT16, citronellol, geraniol, and nerol) from 1 to 100 μM (VvGT14a and VvGT15a to VvGT15c) or 50 to 500 μM (VvGT16) and a fixed UDP-Glc concentration of 108 μM (100 μM unlabeled UDP-Glc and 8 μM UDP-[^{14}C]Glc; VvGT14a), 833 μM (825 μM unlabeled UDP-Glc and 8 μM UDP-[^{14}C]Glc; VvGT15a to VvGT15c), or 512.5 μM (500 μM unlabeled UDP-Glc and 12.5 μM UDP-[^{14}C]Glc; VvGT16). The total volume was 40 μL and 0.2 μg (VvGT14a), 0.5 μg (VvGT15a to VvGT15c), or 5 μg (VvGT16) of purified protein. The measurements were performed under the following conditions. The assays were carried out at 30°C for 1.5 h using Tris-HCl buffer (100 mM, pH 8.5, with 10 mM 2-mercaptoethanol, for VvGT14a and VvGT16). The assay of VvGT15a to VvGT15c was performed at 30°C using Tris-HCl buffer (100 mM, pH 7.5, with 10 mM 2-mercaptoethanol) and 10 min (VvGT15c) or 30 min (VvGT15a and VvGT15b) of incubation for the best substrates. The amount of the purified enzyme and the incubation time were adapted depending on the counting sensibility. The reaction was stopped by adding 1 μL of 24% (v/v) TCA, and glucosides were extracted with 100 μL of ethyl acetate. Radioactivity was determined by LSC. To determine the kinetic data of UDP-Glc, the value of geraniol was fixed (1.25 mM for VvGT15a to VvGT15c and VvGT16; 0.1 mM for VvGT14a), and UDP-[^{14}C]Glc was mixed with nonradiolabeled UDP-Glc to obtain concentrations ranging from 5 to 100 μM (VvGT14a and VvGT15a to VvGT15c) or 25 to 500 μM (VvGT16). The K_m and V_{max} values were calculated from Lineweaver-Burk plots, Hanes-Woolf plots, and nonlinear fitting of the experimental data.

Preparation of Aglycone Libraries

For the preparation of aglycone extracts, 50 g (fresh weight) of grape skins or 4 g (fresh weight) of inflorescences of 'Gewurztraminer 11-18 Gm' was ground to a fine powder in liquid nitrogen. The isolation of glycosides was carried out as described above for metabolite analysis. The methanolic fraction, which was obtained after solid-phase extraction, was enzymatically hydrolyzed. Therefore, the dried sample was dissolved in citric acid buffer (0.1 M, pH 4), and 50 mg of AR 2000 (DSM Food Specialties Beverage Ingredients) was added and incubated for 24 h with exclusion of light. The liberated aglycones were extracted by 20 mL of methyl-*tert*-butyl ether, and the organic phase was reduced to 1,000 μL using a gentle stream of nitrogen.

Activity-Based Profiling Using a Physiologic Aglycone Library

Aliquots of this aglycone extract were incubated with UDP-Glc and various VvGT enzymes. Optimum conditions at 30°C for 24 h were applied. Each

solution contained 100 μL of purified enzyme, 100 to 150 μL of Tris-HCl buffer (100 mM, pH 7.5 or 8.5, with 10 mM 2-mercaptoethanol), 37 pmol of UDP-[^{14}C]Glc (0.01 μCi), and 50 to 100 μL of extract (dissolved in methyl-*tert*-butyl ether). The buffer was mixed with the extract, and the organic solvent was gently vaporized with nitrogen. The missing volume was adjusted with buffer before the enzyme was added. The reaction was stopped by adding 1 μL of 24% (v/v) TCA and extracted with 500 μL of ethyl acetate. After termination of the reaction, free aglycones, which were not converted by VvGT14 and VvGT15, were measured via solid-phase microextraction (SPME)-GC-MS. These residual, free aglycones were completely removed by extraction with dichloromethane. Enzymatically formed glucosides were extracted by ethyl acetate, which was removed under nitrogen. The residue was dissolved in methanol and analyzed by LC-MS/MS to detect the generated monoterpenol glucosides. Enzymatic hydrolysis of the glucosides was performed using AR 2000 and 2 mL of citric acid buffer. After hydrolysis, a 100-μL aliquot was used to detect volatile aglycones via SPME-GC-MS. The remaining solution was extracted with methyl-*tert*-butyl ether and reduced under nitrogen to approximately 200 μL. One microliter was measured by GC-MS via liquid injection.

Enantioselectivity of VvGT14a and VvGT15a to VvGT15c

To determine the enantioselectivity of VvGT14 and VvGT15, the enantiomeric ratio of glucosidically bound citronellol and linalool was determined by enantioselective GC-MS. Following the incubation, residual citronellol and linalool were completely removed by extraction with dichloromethane. Citronellyl β-D-glucoside that remained in the aqueous phase was hydrolyzed by HCl (2 mL, 0.1 M, pH 1) for 1 h at 100°C to release citronellol (Skouroumounis and Sefton, 2000). In the case of linaloyl β-D-glucoside, an enzymatic hydrolysis (AR 2000; citric acid buffer, pH 4, 24 h) was applied due to the instability of linalool in acid solutions (Williams et al., 1982). Hydrolysis of a synthetic 1:1 mixture of *R*- and *S*-linaloyl β-D-glucoside revealed that AR 2000 does not discriminate between the two diastereomeric glucosides. After hydrolysis, citronellol and linalool were analyzed by SPME-GC-MS as described above.

HPLC-MS/MS Analysis

For HPLC-MS/MS analysis of monoterpenyl β-D-glucosides, a Shimadzu LC20AD HPLC system coupled to an API 2000 (Applied Biosystems, AB Sciex) triple-quadrupole mass spectrometer was used. Data acquisition was performed using Analyst software version 1.6.1. (Applied Biosystems, AB Sciex). The column (Phenomenex Gemini-NX 5u C18, 250 × 3 mm) was eluted with a linear gradient starting at water:acetonitrile (7:3, v/v) containing 0.2% (v/v) ammonia at 12 min to water:acetonitrile (4:6, v/v; 0.2% (v/v) ammonia) at 18 min. The column temperature was maintained at 40°C. The mass spectrometer was operated in electrospray ionization (ESI)-multiple reaction monitoring (MRM) negative ion mode. Nitrogen was used as curtain (setting, 20), nebulizing, and collision gas (collision energy was −20 eV). Monoterpenyl β-D-glucosides were identified by the following characteristic MRM transitions: linaloyl glucoside, mass-to-charge ratio (*m/z*) 315→161(Glu), 315→113(Glu); neryl glucoside, *m/z* 315→119(Glu), 315→113(Glu); geranyl glucoside, *m/z* 315→119(Glu), 315→113(Glu); citronellyl glucoside, *m/z* 317→101(Glu), 317→161(Glu) [Domon and Costello, 1988; Cole et al., 1989; Salles et al., 1991; Supplemental Table S3].

GC-MS Analysis

GC-MS analysis was performed with a Varian GC-450 coupled to a Varian MS-240 ion trap employing a Phenomenex Zebron ZB-WAXplus column (30 m × 0.25 mm × 0.25 μm). Helium flow rate was 1 mL min^{-1}. The analysis was carried out in split mode (liquid injections) or splitless mode (SPME measurements) with 220°C injector temperature. Transfer line temperature was 230°C. Electron impact ionization-mass spectra were recorded from *m/z* 40 to 300 (ionization energy, 70 eV; trap temperature, 170°C). The oven temperature program was 60°C (3 min) and 10°C min^{-1} to 250°C (5 min). In the case of SPME measurements, liberated aglycones were isolated for 10 min at 60°C using a fiber coated with an 85-μm film of polyacrylate (Supelco). After extraction, the SPME fiber was desorbed for 10 min at 250°C in the injection port of the GC-MS system and the column oven program was carried out as described above. Enantioselective GC-MS analysis was performed with a Varian GC-450 coupled to a Varian MS-240 ion trap. The column was a DiAcß [heptakis-(2,3-di-*O*-acetyl-6-*O*-*tert*-butyldimethylsilyl)-β-cyclodextrin], 26 m × 0.32 mm i.d. with 0.1-μm film. Helium was used as the carrier gas at a flow rate of 1 mL min^{-1}, injector temperature was 250°C, with a split ratio of 1:100 (liquid injections) or splitless (SPME measurements). The oven temperature program was 70°C (3 min), 0.5°C min^{-1} to 130°C, and 20°C min^{-1} to 200°C (3 min). The transfer line temperature was 230°C. GC-MS measurements were recorded in full-scan mode. Selected ion monitoring mode was used for quantification.

Radio-TLC Analysis

Assays containing UDP-[^{14}C]Glc and aglycone libraries or substrates were performed as described above and subsequently extracted with 500 μL of ethyl acetate. The organic solvent was vaporized, and the pellet was resuspended in 10 μL of methanol and was applied on Silica Gel 60 F254 plates (Merck). The dried plates were developed in a solvent system of chloroform: acetic acid:water (50:45:5, v/v/v). The plates were dried and analyzed by digital autoradiography (EG&G Berthold).

Sequence data from this article can be found in the GenBank/EMBL data libraries under accession numbers VvGT14 (*VIT_18s0001g06060* [*XM_002285734.2*; XP_002285770.1]); VvGT15 (*VIT_06s0004g05780* [*XM_002281477.2*; XP_002281513.2]); VvGT16 (*VIT_3s0017g01130* [*XM_002263122.1*; XP_002263158.1]); VvGT17 (*VIT_8s0001g05950* [*XM_002285743.2*; XP_002285779.1]); VvGT18 (*VIT_3s0180g00280* [*XM_002285372.1*; XP_002285408.1]); VvGT19 (*VIT_8s0001g05910* [*XM_002285744.1*; *XP_002285780.1*]); VvGT20 (*VIT_05s0062g00430* [*XM_002266592.2*; XP_002266628.1]).

Supplemental Data

The following materials are available in the online version of this article.

Supplemental Figure S1. Locations of putative UGT genes.

Supplemental Figure S2. Gene expression analysis of *VvGTs* by GeXP in nonberry tissues.

Supplemental Figure S3. Gene expression analysis of *VvGTs* by GeXP during berry development.

Supplemental Figure S4. Gene expression analysis of *VvGTs* by GeXP during two consecutive years.

Supplemental Figure S5. SDS-PAGE and western-blot analysis VvGT14 and VvGT16.

Supplemental Figure S6. SDS-PAGE and western-blot analysis VvGT15.

Supplemental Figure S7. Radio-TLC analysis of products formed by VvGT14 and VvGT16.

Supplemental Figure S8. Radio-TLC analysis of products formed by VvGT15.

Supplemental Figure S9. Multiple protein sequence alignment of the three variants of VvGT14.

Supplemental Figure S10. Enantiomeric discrimination of VvGT enzymes.

Supplemental Table S1. Gene-specific primers used for GeXP.

Supplemental Table S2. Primers used in PCR for subsequent cloning and sequencing.

Supplemental Table S3. MRM transitions and excitation voltage of the ESI-MS/MS method.

Supplemental Table S4. Response factor calculation by GC-MS (total ion chromatogram, *m/z* 40–300)

ACKNOWLEDGMENTS

We thank Thomas Hoffmann for help during LC-MS analysis.

Received May 8, 2014; accepted July 28, 2014; published July 29, 2014.

LITERATURE CITED

Bönisch F, Frotscher J, Stanitzek S, Rühl E, Wüst M, Bitz O, Schwab W (2014) A UDP-glucose:monoterpenol glucosyltransferase adds to the chemical diversity of the grapevine metabolome. Plant Physiol **165:** 561–581

Bowles D, Lim EK, Poppenberger B, Vaistij FE (2006) Glycosyltransferases of lipophilic small molecules. Annu Rev Plant Biol **57:** 567–597

Caputi L, Lim EK, Bowles DJ (2008) Discovery of new biocatalysts for the glycosylation of terpenoid scaffolds. Chemistry **14:** 6656–6662

Caputi L, Lim EK, Bowles DJ (June 10, 2010) Monoterpenoid modifying enzymes. US Patent Application No. US2010/0143975

Caputi L, Malnoy M, Goremykin V, Nikiforova S, Martens S (2012) A genome-wide phylogenetic reconstruction of family 1 UDP-glycosyltransferases revealed the expansion of the family during the adaptation of plants to life on land. Plant J **69:** 1030–1042

Cole RB, Tabet JC, Salles C, Crouzet J (1989) Structural "memory effects" influencing decompositions of glucose alkoxide anions produced from monoterpene glycoside isomers in tandem mass spectrometry. Rapid Commun Mass Spectrom **3:** 59–61

de Carvalho LPS, Zhao H, Dickinson CE, Arango NM, Lima CD, Fischer SM, Ouerfelli O, Nathan C, Rhee KY (2010) Activity-based metabolomic profiling of enzymatic function: identification of Rv1248c as a mycobacterial 2-hydroxy-3-oxoadipate synthase. Chem Biol **17:** 323–332

Domon B, Costello CE (1988) A systematic nomenclature for carbohydrate fragmentations in FAB-MS/MS spectra of glycoconjugates. Glycoconjugate **5:** 397–409

Duckworth BP, Aldrich CC (2010) Assigning enzyme function from the metabolic milieu. Chem Biol **17:** 313–314

Ford CM, Hoj P (1998) Multiple glucosyltransferase activities in grapevine *Vitis vinifera* L. Aust J Grape Wine Res **4:** 48–58

Gunata YZ, Bayonove CL, Tapiero C, Cordonnier RE (1990) Hydrolysis of grape monoterpenyl β-D-glucosides by various β-glucosidases. J Agric Food Chem **38:** 1232–1236

Gunata Z, Bitteur SM, Brillouet JM, Bayonove CL, Cordonnier R (1988) Sequential enzymic hydrolysis of potentially aromatic glycosides from grape. Carbohydr Res **184:** 139–149

Hansen KS, Kristensen C, Tattersall DB, Jones PR, Olsen CE, Bak S, Møller BL (2003) The in vitro substrate regiospecificity of recombinant UGT85B1, the cyanohydrin glucosyltransferase from *Sorghum bicolor*. Phytochemistry **64:** 143–151

Hattori S, Kawaharada C, Tazaki H, Fujimori T, Kimura K, Ohnishi M, Nabeta K (2004) Formation mechanism of 2,6-dimethyl-2,6-octadienes from thermal decomposition of linalyl β-D-glucopyranoside. Biosci Biotechnol Biochem **68:** 2656–2659

He XZ, Wang X, Dixon RA (2006) Mutational analysis of the Medicago glycosyltransferase UGT71G1 reveals residues that control regioselectivity for (iso)flavonoid glycosylation. J Biol Chem **281:** 34441–34447

Hill RK, Abächerli C, Hagishita S (1994) Synthesis of (2*S*,4*S*)- and (2*S*,4*R*)-[5,5,5-$^2H_3$]leucine from (R)-pulegone. Can J Chem **72:** 110–113

Hughes J, Hughes MA (1994) Multiple secondary plant product UDP-glucose glucosyltransferase genes expressed in cassava (*Manihot esculenta* Crantz) cotyledons. DNA Seq **5:** 41–49

Jaillon O, Aury JM, Noel B, Policriti A, Clepet C, Casagrande A, Choisne N, Aubourg S, Vitulo N, Jubin C, et al (2007) The grapevine genome sequence suggests ancestral hexaploidization in major angiosperm phyla. Nature **449:** 463–467

Jánváry L, Hoffmann T, Pfeiffer J, Hausmann L, Töpfer R, Fischer TC, Schwab W (2009) A double mutation in the anthocyanin 5-O-glucosyltransferase gene disrupts enzymatic activity in *Vitis vinifera* L. J Agric Food Chem **57:** 3512–3518

Jesús Ibarz M, Ferreira V, Hernández-Orte P, Loscos N, Cacho J (2006) Optimization and evaluation of a procedure for the gas chromatographic-mass spectrometric analysis of the aromas generated by fast acid hydrolysis of flavor precursors extracted from grapes. J Chromatogr A **1116:** 217–229

Khater F, Fournand D, Vialet S, Meudec E, Cheynier V, Terrier N (2012) Identification and functional characterization of cDNAs coding for hydroxybenzoate/hydroxycinnamate glucosyltransferases co-expressed with genes related to proanthocyanidin biosynthesis. J Exp Bot **63:** 1201–1214

Konda Y, Toida T, Kaji E, Takeda K, Harigaya Y (1997) First total synthesis of two new diglycosides, neohancosides A and B, from *Cynanchum hancockianum*. Carbohydr Res **301:** 124–143

Luan F, Hampel D, Mosandl A, Wüst M (2004) Enantioselective analysis of free and glycosidically bound monoterpene polyols in *Vitis vinifera* L. cvs. Morio Muscat and Muscat Ottonel: evidence for an oxidative monoterpene metabolism in grapes. J Agric Food Chem **52:** 2036–2041

Luan F, Mosandl A, Münch A, Wüst M (2005) Metabolism of geraniol in grape berry mesocarp of *Vitis vinifera* L. cv. Scheurebe: demonstration of stereoselective reduction, E/Z-isomerization, oxidation and glycosylation. Phytochemistry **66:** 295–303

Lücker J, Bouwmeester HJ, Schwab W, Blaas J, van der Plas LHW, Verhoeven HA (2001) Expression of Clarkia S-linalool synthase in transgenic petunia plants results in the accumulation of S-linalyl-β-D-glucopyranoside. Plant J **27:** 315–324

Marais J (1983) Terpenes in the aroma of grapes and wines: a review. S Afr J Enol Vitic **4:** 49–58

Masada S, Terasaka K, Mizukami H (2007) A single amino acid in the PSPG-box plays an important role in the catalytic function of CaUGT2 (curcumin glucosyltransferase), a group D family 1 glucosyltransferase from *Catharanthus roseus*. FEBS Lett **581:** 2605–2610

Mateo JJ, Jiménez M (2000) Monoterpenes in grape juice and wines. J Chromatogr A **881:** 557–567

Offen W, Martinez-Fleites C, Yang M, Kiat-Lim E, Davis BG, Tarling CA, Ford CM, Bowles DJ, Davies GJ (2006) Structure of a flavonoid glucosyltransferase reveals the basis for plant natural product modification. EMBO J **25:** 1396–1405

Ono E, Homma Y, Horikawa M, Kunikane-Doi S, Imai H, Takahashi S, Kawai Y, Ishiguro M, Fukui Y, Nakayama T (2010) Functional differentiation of the glycosyltransferases that contribute to the chemical diversity of bioactive flavonol glycosides in grapevines (*Vitis vinifera*). Plant Cell **22:** 2856–2871

Osmani SA, Bak S, Møller BL (2009) Substrate specificity of plant UDP-dependent glycosyltransferases predicted from crystal structures and homology modeling. Phytochemistry **70:** 325–347

Paulsen H, Le-Nguyén B, Sinnwell V, Heemann V, Seehofer F (1985) Synthesis of glycosides of mono-, sesqui- and diterpene alcohols. Eur J Org Chem **8:** 1513–1536

Piñeiro Z, Palma M, Barroso CG (2004) Determination of terpenoids in wines by solid phase extraction and gas chromatography. Anal Chim Acta **513:** 209–214

Reid KE, Olsson N, Schlosser J, Peng F, Lund ST (2006) An optimized grapevine RNA isolation procedure and statistical determination of reference genes for real-time RT-PCR during berry development. BMC Plant Biol **6:** 27

Salles C, Jallageas JC, Beziat Y, Cristau HJ (1991) Synthesis of 4- and 10-deuterated neryl and geranyl-β-D-glucosides and their use in corroboration of a mechanism proposed for the fragmentation of heterosides in tandem mass spectrometry. J Labelled Comp Radiopharm **31:** 11–22

Schwab W (2003) Metabolome diversity: too few genes, too many metabolites? Phytochemistry **62:** 837–849

Sefton M, Francis IL, Williams PJ (1996) Free and bound volatile secondary metabolites of *Vitis vinifera* grape cv. Sauvignon Blanc. J Food Sci **59:** 142–147

Skouroumounis GK, Sefton MA (2000) Acid-catalyzed hydrolysis of alcohols and their β-D-glucopyranosides. J Agric Food Chem **48:** 2033–2039

Strauss UT, Felfer U, Faber K (1999) Biocatalytic transformation of racemates into chiral building blocks in 100% chemical yield and 100% enantiomeric excess. Tetrahedron Asymmetry **10:** 107–117

Voirin SG, Baumes R, Bitteur SM, Gunata Z, Bayonove C (1990) Novel monoterpene disaccharide glycosides of *Vitis vinifera* grapes. J Agric Food Chem **38:** 1373–1378

Williams PJ, Strauss CR, Wilson B, Massy-Westropp RA (1982) Studies on the hydrolysis of *Vitis vinifera* monoterpene precursor compounds and model monoterpene β-D-glucosides rationalizing the monoterpene composition of grapes. J Agric Food Chem **30:** 1219–1223

Wilson B, Strauss CR, Williams PJ (1984) Changes in free and glycosidically bound monoterpenes in developing Muscat grapes. J Agric Food Chem **32:** 919–924

Wilson B, Strauss CR, Williams PJ (1986) The distribution of free and glycosidically bound monoterpenes among skin, juice, and pulp fractions of some white grape varieties. Am J Enol Vitic **37:** 107–111

Wirth J, Guo W, Baumes R, Günata Z (2001) Volatile compounds released by enzymatic hydrolysis of glycoconjugates of leaves and grape berries from *Vitis vinifera* Muscat of Alexandria and Shiraz cultivars. J Agric Food Chem **49:** 2917–2923

Wüst M, Rexroth A, Beck T, Mosandl A (1998) Mechanistic aspects of the biogenesis of rose oxide in *Pelargonium graveolens* L'Héritier. Chirality **10:** 229–237

Ye J, Coulouris G, Zaretskaya I, Cutcutache I, Rozen S, Madden TL (2012) Primer-BLAST: a tool to design target-specific primers for polymerase chain reaction. BMC Bioinformatics **13:** 134

Yonekura-Sakakibara K, Hanada K (2011) An evolutionary view of functional diversity in family 1 glycosyltransferases. Plant J **66:** 182–193

Zeng Y, Yang T (2002) RNA isolation from highly viscous samples rich in polyphenols and polysaccharides. Plant Mol Biol Rep **20:** 417